REPORT No. 718

PRESSURE DISTRIBUTION OVER AN NACA 23021 AIRFOIL WITH A SLOTTED AND A SPLIT FLAP

By THOMAS A. HARRIS and JOHN G. LOWRY

SUMMARY

A pressure-distribution investigation has been conducted in the NACA 4- by 6-foot vertical wind tunnel to determine the air loads on an NACA 23021 airfoil in combination with a 25.66-percent-chord slotted flap and a 20-percent-chord split flap. Pressures were measured on both the upper and the lower surfaces of the main airfoil and the flaps for several angles of attack and at several flap settings.

The data, presented as pressure diagrams and as graphs of the section coefficients for the flap alone and for the airfoil-flap combinations, are applicable to rib and flap design for a combination of a thick airfoil and a slotted or a split flap. The results of previous tests of an NACA 23012 airfoil with a slotted flap are compared with the present results. This comparison showed: The flap normal-force coefficients were approximately the same at high angles of attack. The flap pitching-moment coefficients were approximately the same for the range tested. The chord-force coefficients for the flap on the NACA 23021 airfoil were generally slightly higher than for the flap on the NACA 23012 airfoil. The results for the split flap were about the same as for previous tests of split flaps on thinner airfoils.

INTRODUCTION

The National Advisory Committee for Aeronautics is undertaking an extensive investigation of various airfoil-flap combinations to furnish information applicable to the aerodynamic and the structural design of high-lift devices intended to increase the safety and the performance of airplanes. One of the promising arrangements is an airfoil in combination with a slotted flap. Data are available for aerodynamic and structural design of 12-percent-thick airfoils in combination with a slotted flap, but little data are available for the design of combinations of thick airfoils and flaps. The present investigation was conducted to add load data to the aerodynamic data already available (reference 1) and to extend the data for loads on slotted flaps (references 2 and 3).

Some form of split flap is commonly used at present. Aerodynamic information is available for the split flap in combination with airfoils of several thicknesses (reference 4); but most of the load data for wing-flap combinations are for thin airfoils, such as the Clark Y and the NACA 2212 (references 5, 6, and 7). The present investigation will furnish load data for the split flap in combination with a thick airfoil.

The present pressure-distribution tests were made of an NACA 23021 airfoil in combination with the 25.66-percent-chord slotted flap 2-b (reference 1) and the 20-percent-chord split flap (reference 4). Tests were made at various angles of attack and flap settings.

APPARATUS AND TESTS

MODELS

The airfoil model used in these tests had a 4-foot span and a 3-foot chord; it conformed to the NACA 23021 airfoil profile and was constructed of laminated mahogany with a hollow section to accommodate the copper pressure tubes. The basic model, which consisted of the airfoil in combination with a full-span slotted flap (fig. 1), was furnished with a mahogany filler block which fitted the slot entry in the lower surface so that a smooth airfoil was formed. The slotted flap was attached to the airfoil by two hinges located on the tips of the airfoil. The full-span split flap was constructed of quarter-inch plywood and was attached to the airfoil by several braces equally spaced along the span.

The full-span slotted flap (fig. 1 (a)) was developed by the NACA and is designated 2-b in reference 1. It has a chord of 9.238 inches (25.66 percent of the over-all airfoil chord). A full-span metal lip located on the upper-surface trailing edge of the airfoil acts as a partial seal when the flap is undeflected and directs the flow of air over the deflected flap. The path of the flap nose (fig. 1) is the optimum one reported in reference 1, where the nose of the flap was defined as the point of tangency of a line normal to the airfoil chord and tangent to the leading edge of the flap in its neutral position. The flap was arranged for locking at downward, or positive, flap directions.

The split flap (fig. 1 (b)) has a chord of 7.20 inches (20 percent of the over-all airfoil chord). The leading edge was sealed with plasticine for all tests to prevent any leakage. The flap was arranged for locking at downward, or positive, flap deflections. The flap angles were measured from the lower surface of the airfoil as shown in figure 1 (b).

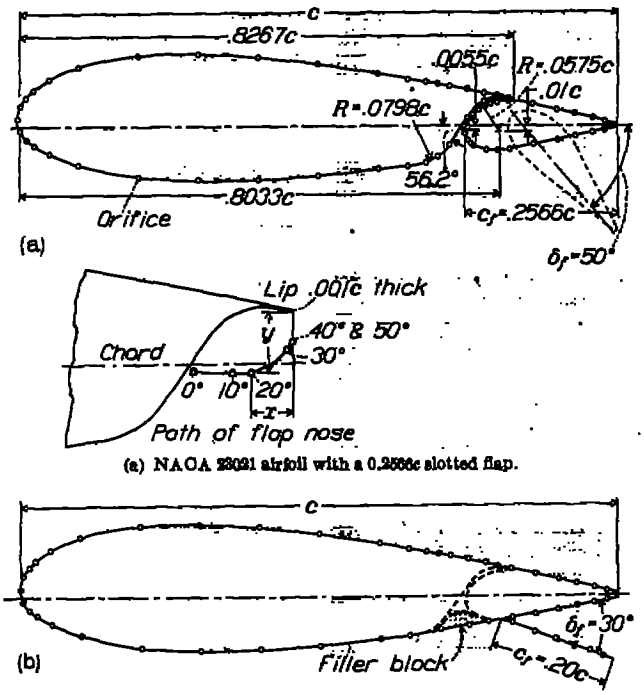

(a) NACA 23021 airfoil with a 0.2566c slotted flap.

(b) NACA 23021 airfoil with a 0.20c split flap.

	δ_f (deg)	0	10	20	30	40	50
Path of flap nose for various flap deflections. Distances are measured from lower edge of lip in percent c	x	8.33	5.0	3.5	0.5	0	0
	y	4.85	5.0	5.0	3.0	2.5	2.5

FIGURE 1.—Cross section of model showing airfoil-flap combinations used in pressure-distribution tests.

The model was fitted with a single chordwise row of pressure orifices at the midspan located as shown in table I and figure 1. A single row was used because the results of the tests of reference 8 showed one to be sufficient. Tubes leading from these orifices were brought out through one end of the wing (fig. 2) and connected to a multiple-tube photographically recording manometer.

TABLE I.—ORIFICE LOCATIONS ON AIRFOIL-FLAP COMBINATIONS TESTED

NACA 23021 36-inch airfoil with a 0.2566c slotted flap				NACA 23021 36-inch airfoil with a 0.20c split flap			
Orifice locations on upper and lower surfaces of airfoil in percentage chord from leading edge of airfoil		Orifice locations on upper and lower surfaces of flap in percentage flap chord from leading edge of flap		Orifice locations on upper and lower surfaces of airfoil in percentage chord from leading edge of airfoil		Orifice locations on upper and lower surfaces of flap in percentage flap chord from leading edge of flap	
Orifice	Location	Orifice	Location	Orifice	Location	Orifice	Location
0	0	0	0	0	0	-----	-----
1	.25	1	.63	1	.25	1	10.00
2	1.25	2	2.58	2	1.25	2	30.00
3	2.50	3	4.53	3	2.50	3	50.00
4	5.00	4	6.47	4	5.00	4	80.00
5	10.00	5	*10.38	5	10.00	5	90.00
6	20.00	6	14.26	6	20.00	-----	-----
7	30.00	7	*18.16	7	30.00	-----	-----
8	40.00	8	22.06	8	40.00	-----	-----
9	50.00	9	28.86	9	50.00	-----	-----
10	60.00	10	45.45	10	60.00	-----	-----
11	65.00	11	61.01	11	65.00	-----	-----
12	68.00	12	72.72	12	*68.00	-----	-----
13	70.00	13	84.41	13	70.00	-----	-----
14	72.00	14	92.20	14	*72.00	-----	-----
15	75.00	-----	-----	15	75.00	-----	-----
16	78.00	-----	-----	16	78.00	-----	-----
17	80.00	-----	-----	17	*80.00	-----	-----
18	82.00	-----	-----	18	82.00	-----	-----
-----	-----	-----	-----	19	86.00	-----	-----
-----	-----	-----	-----	20	90.00	-----	-----
-----	-----	-----	-----	21	93.00	-----	-----
-----	-----	-----	-----	22	96.00	-----	-----
-----	-----	-----	-----	23	98.00	-----	-----

* Upper surface only.

TEST INSTALLATION

The model was mounted in the closed test section of the NACA 4- by 6-foot vertical wind tunnel (references 9 and 10). Because the model completely spanned the tunnel except for small clearances at each end (fig. 2), the sides of the tunnel acted as end plates and approximately two-dimensional flow was obtained. Torque tubes attached to the balance frame held the model rigidly and also served as a conduit for the pressure

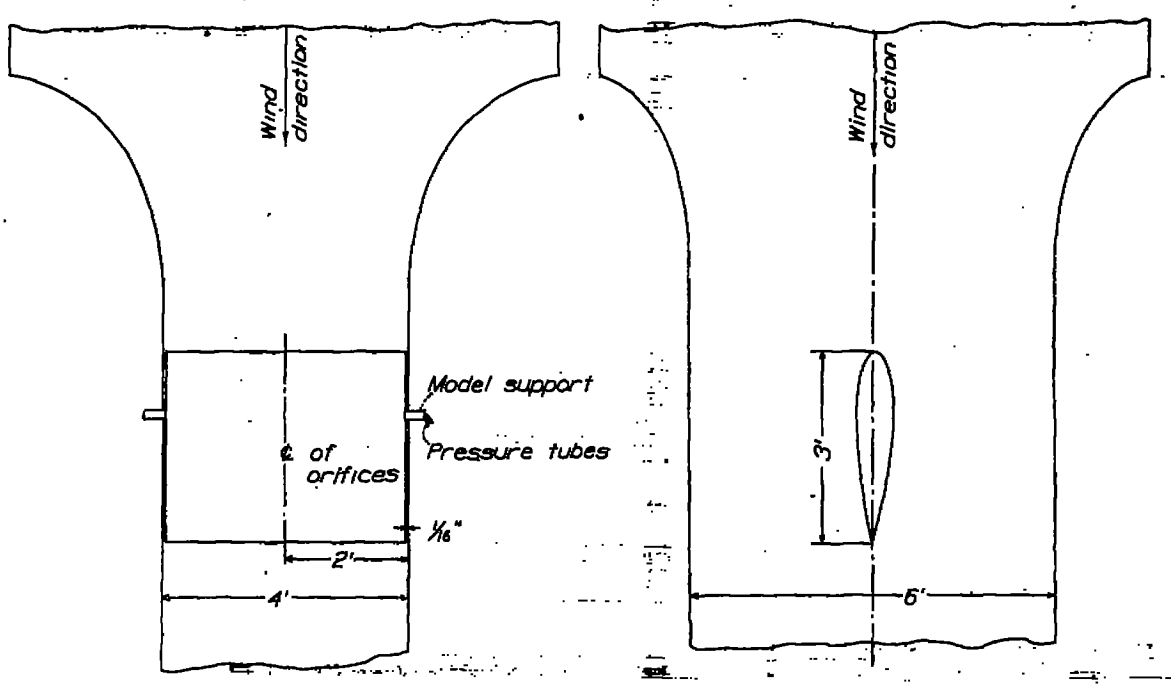

FIGURE 2.—Model installation in the 4- by 6-foot vertical wind tunnel.

tubes. The angle of attack was set from outside the tunnel by rotating the torque tubes with a calibrated electric drive.

TESTS

The tests were run at an average dynamic pressure of 11.05 pounds per square foot, corresponding to an airspeed of approximately 65 miles per hour and to an average test Reynolds number, based on the chord of the airfoil with flap fully retracted, of about 1,840,000. The effective Reynolds number R_e was about 3,560,000 and is equal to the test Reynolds number multiplied by the turbulence factor, which is 1.93 for the 4- by 6-foot vertical tunnel.

The model was tested with the slotted flap deflected from 0° to 50° in increments of 10° and the split flap deflected from 0° to 75° in 15° increments. The tests were made through an angle-of-attack range from zero to approximately maximum lift in 4° increments.

With the model at a given angle of attack and flap setting, time was allowed for conditions in the tunnel and for the manometer to become stable before the pressures were recorded.

PRESENTATION OF DATA

PRESSURE DIAGRAMS

All the diagrams of pressure over the upper and the lower surfaces of the combination are given as the ratio of the static pressure p at a point, or an orifice, on the airfoil to the free-stream dynamic pressure q for the individual flap and angle-of-attack settings. Pressures over the airfoil in combination with the slotted flap are shown in figures 3 to 13, and pressures over the split-flap combination are shown in figures 14 to 19. A comparison of the loads on the plain airfoil and the loads on the airfoil-flap combinations for the same lift and angle of attack is shown for three flap settings in figures 20 and 21.

In figures 3 to 8, the pressures over the main airfoil are plotted normal to the airfoil chord and the pressures over the slotted flap are plotted normal to the flap reference line. The flap reference line is a line through the nose point of the flap and parallel to the main airfoil chord line with flap neutral. In figures 14 to 19, the pressures over the airfoil and the split flap are plotted normal to the airfoil chord but the flap pressures are plotted from an imaginary flap chord line. This imaginary flap chord line is the deflected-flap chord line moved normal to the airfoil chord line until the leading edge intersects the airfoil chord line. The imaginary flap chord line is not shown because it would only complicate the figures.

COEFFICIENTS

The pressure diagrams were mechanically integrated to obtain data from which standard section coefficients were computed. Where the term "flap alone" is used, it refers to the forces on the flap in the presence of the main portion of the airfoil. The section coefficients are defined as follows:

$c_{n_w}=n_w/qc$ normal-force coefficient of airfoil with flap

$c_{n_f}=n_f/qc_f$ normal-force coefficient of flap alone

$c_{m_w}=m_w/qc^2$ pitching-moment coefficient of airfoil with flap about quarter-chord point of airfoil with flap neutral

$c_{m_f}=m_f/qc_f^2$ pitching-moment coefficient of slotted flap alone about quarter-chord point of flap

$c_{h_f}=h_f/qc_f^2$ hinge-moment coefficient of split flap alone about leading edge (hinge axis) of flap

$c_{c_f}=x_f/qc_f$ chord-force coefficient of slotted flap alone

$(c.\ p.)_w=\left(0.25-\frac{c_{m_w}}{c_{n_w}}\right)\times 100$ center-of-pressure location of airfoil with flap in percentage of airfoil chord from leading edge of airfoil

$(c.\ p.)_f=\left(0.25-\frac{c_{m_f}}{c_{n_f}}\right)\times 100$ center-of-pressure location of slotted flap alone in percentage of flap chord from leading edge of flap

$(c.\ p.)_f=-\frac{c_{h_f}}{c_{n_f}}\times 100$ center-of-pressure location of split flap alone in percentage of flap chord from leading edge of flap

where the forces and moments per unit span are:

n_w normal force on airfoil with flap

n_f normal force on flap alone normal to chord of flap

m_w pitching moment of airfoil with flap

m_f pitching moment of slotted flap alone

h_f hing moment of split flap

x_f chord force on slotted flap

q dynamic pressure of free air stream

c chord of airfoil with flap neutral

c_f chord of flap (measured from nose to tail)

and

α_0 angle of attack for infinite aspect ratio

δ_f angle of flap deflection

The coefficients for the combination were derived from the normal forces alone, the chord forces on the flaps being neglected. In the case of the slotted flap, however, neglecting the normal-force component of the chord force of the flap in the calculations for the combination reduced the values by an average amount of 0.04. Because the skin friction of the flap will enter into any correction for this discrepancy, no attempt was made to include a correction for flap chord force in the final results. Inasmuch as the model completely spanned the jet, the integrated results, which are in coefficient form, may be used as section characteristics.

Figures 22 to 27 show the section characteristics of the combination and of the flap alone for the slotted flap; figures 28 to 33 show the section characteristics of the combination and of the flap alone for the split flap. In figure 28 (b), the forces on the split flap when neutral were found by assuming that the only leakage between flap and airfoil was at the trailing edge; the loads were computed on that basis.

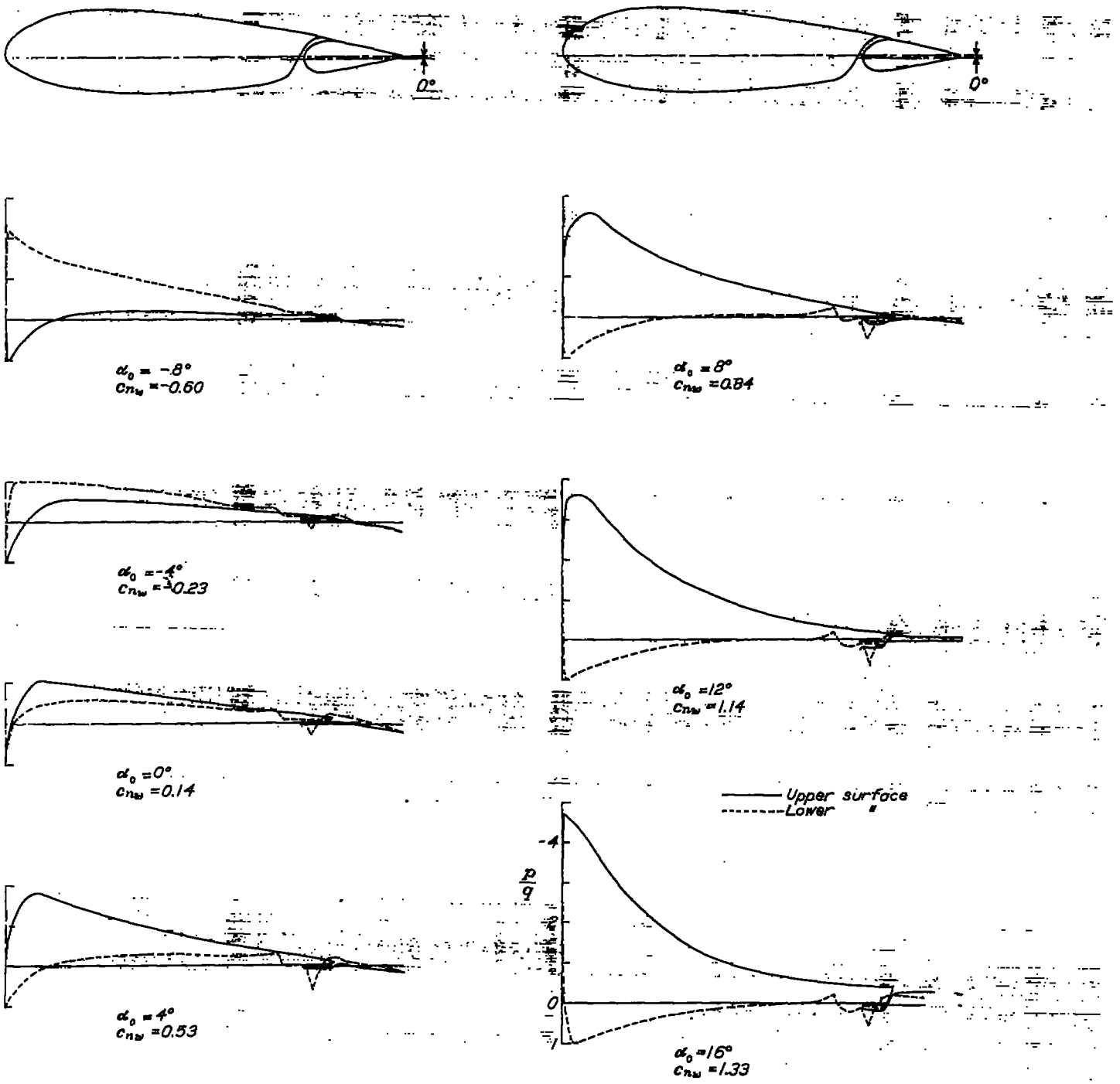

FIGURE 3.—Pressure distribution on the NACA 23021 airfoil with a 0.256c slotted flap at various angles of attack. Flap set at 0°.

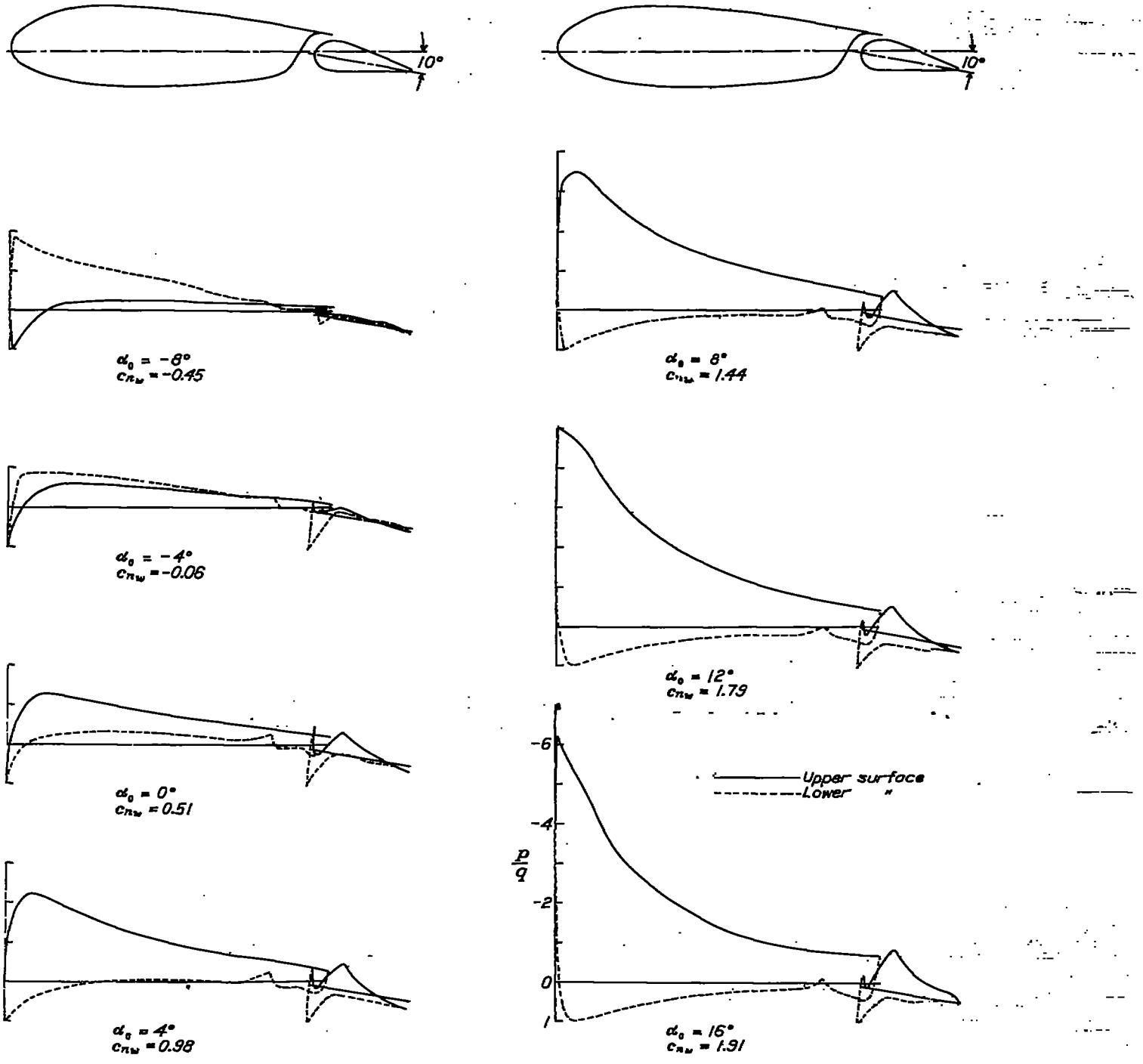

FIGURE 4.—Pressure distribution on the NACA 23021 airfoil with a 0.250c slotted flap at various angles of attack. Flap set at 10°.

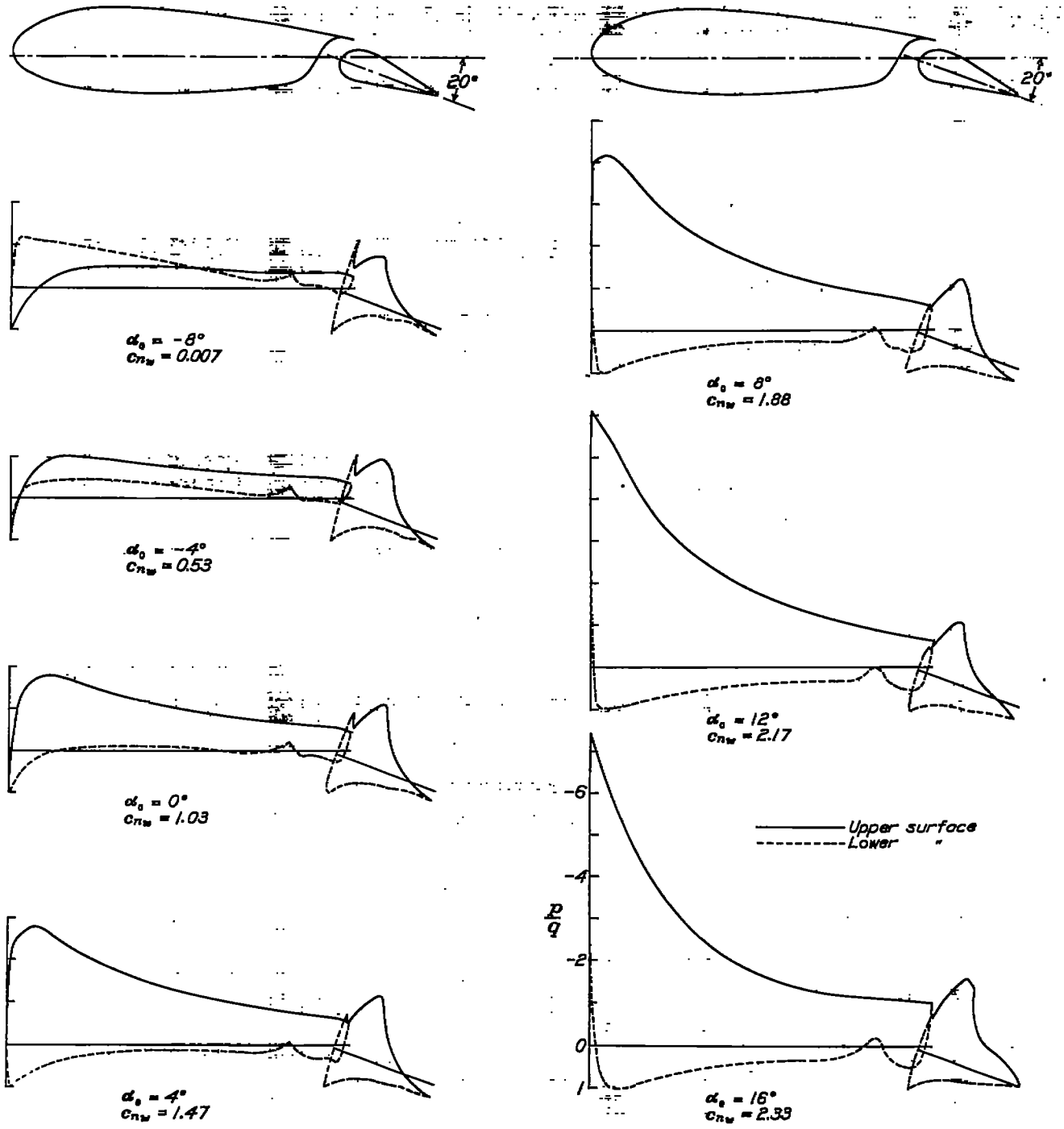

FIGURE 5.—Pressure distribution on the NACA 23021 airfoil with a 0.25$6c$ slotted flap at various angles of attack. Flap set at 20°.

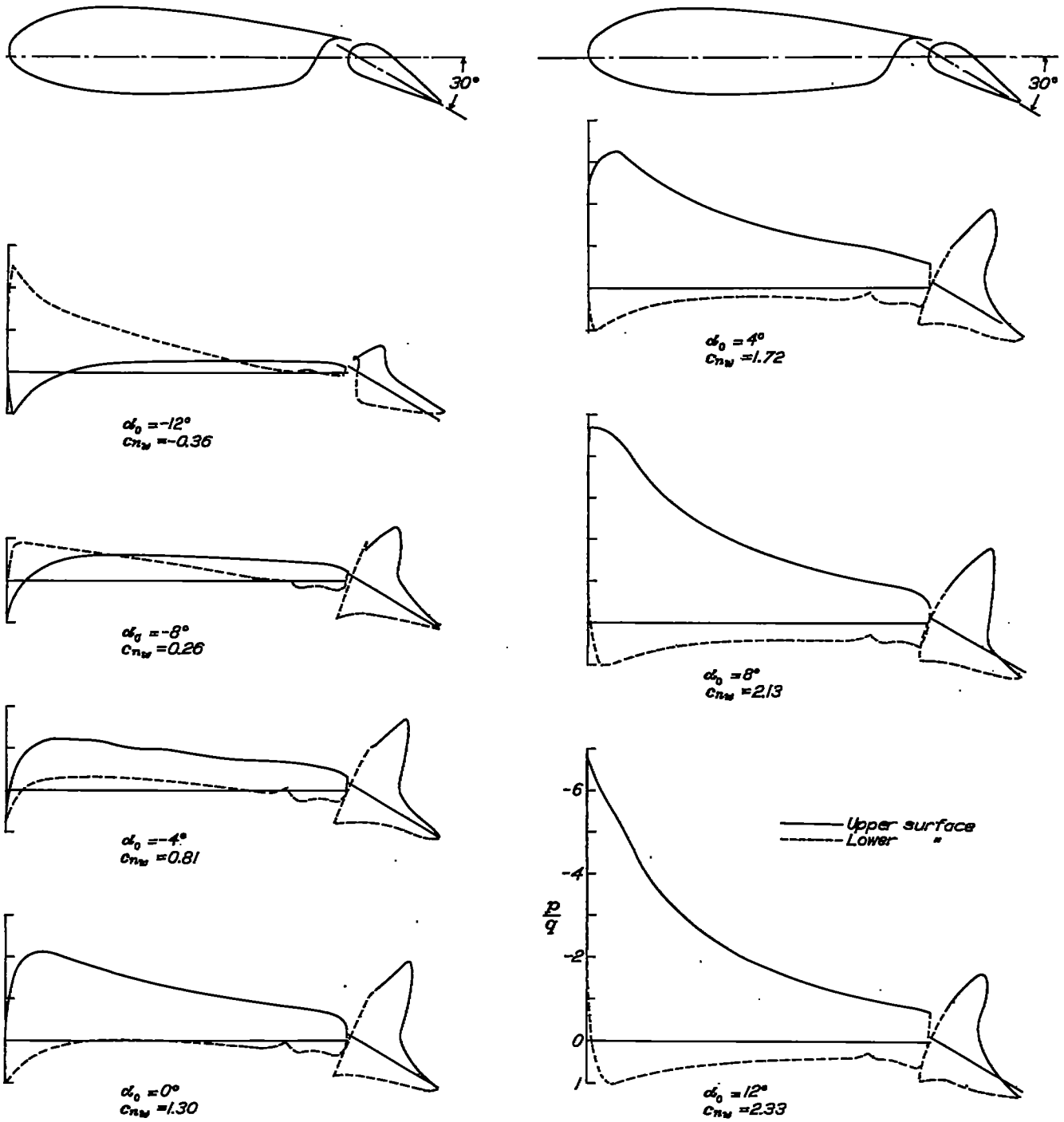

FIGURE 6.—Pressure distribution on the NACA 23021 airfoil with a 0.25$6c$ slotted flap at various angles of attack. Flap set at 30°.

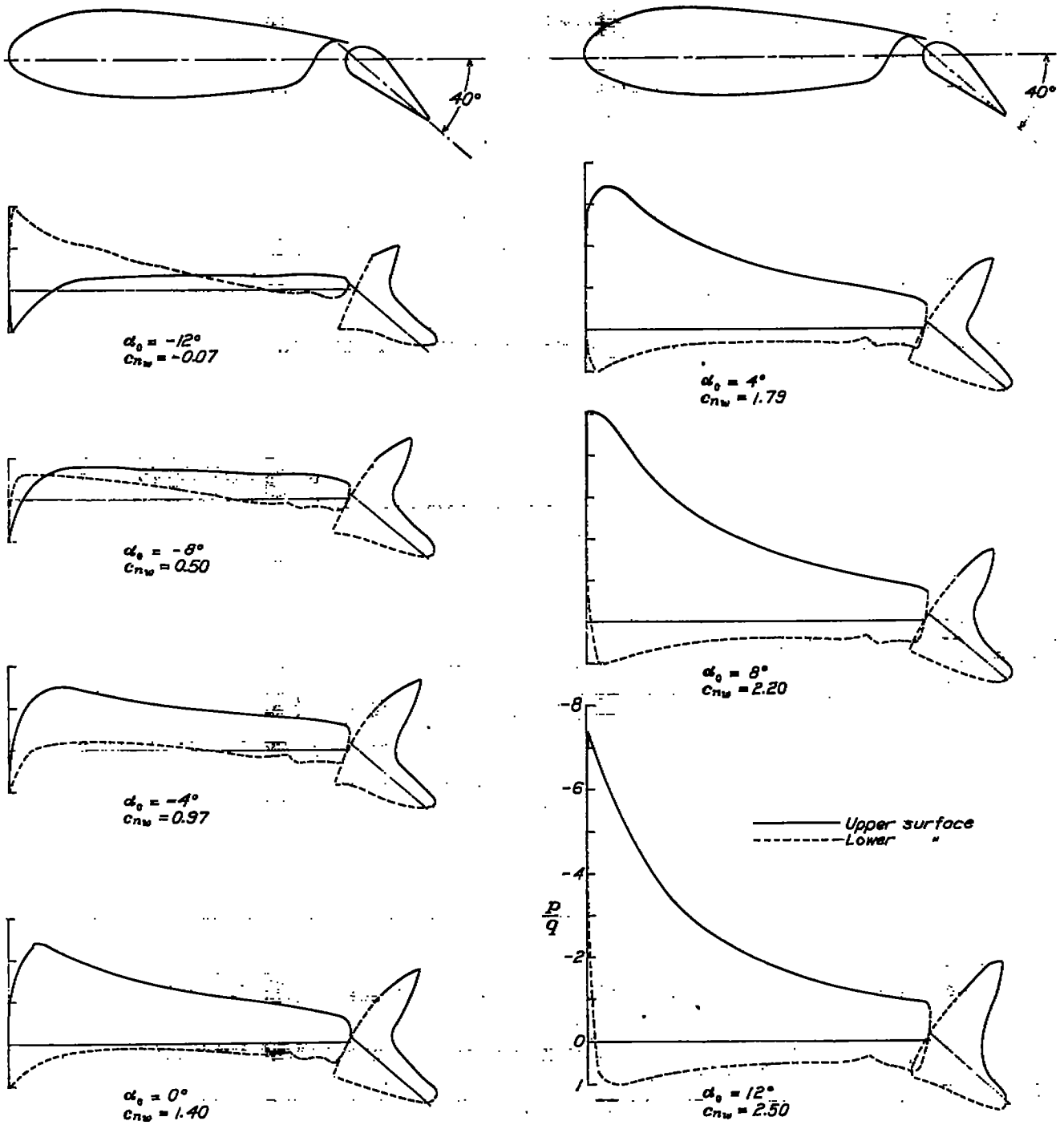

FIGURE 7.—Pressure distribution on the NACA 23021 airfoil with a 0.25$\bar{6}$c slotted flap at various angles of attack. Flap set at 40°.

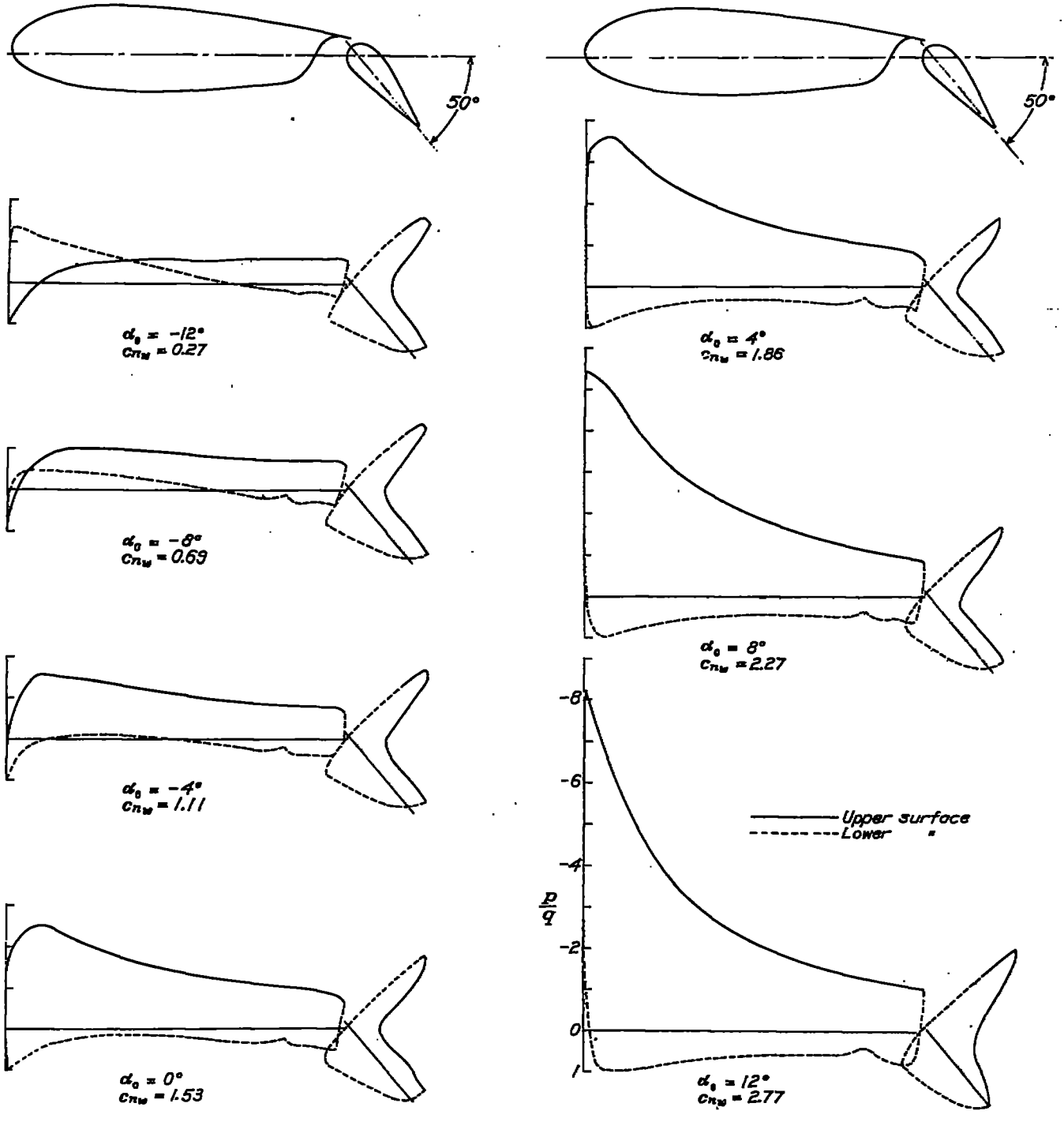

FIGURE 8.—Pressure distribution on the NACA 23021 airfoil with a 0.25$6c$ slotted flap at various angles of attack. Flap set at 50°.

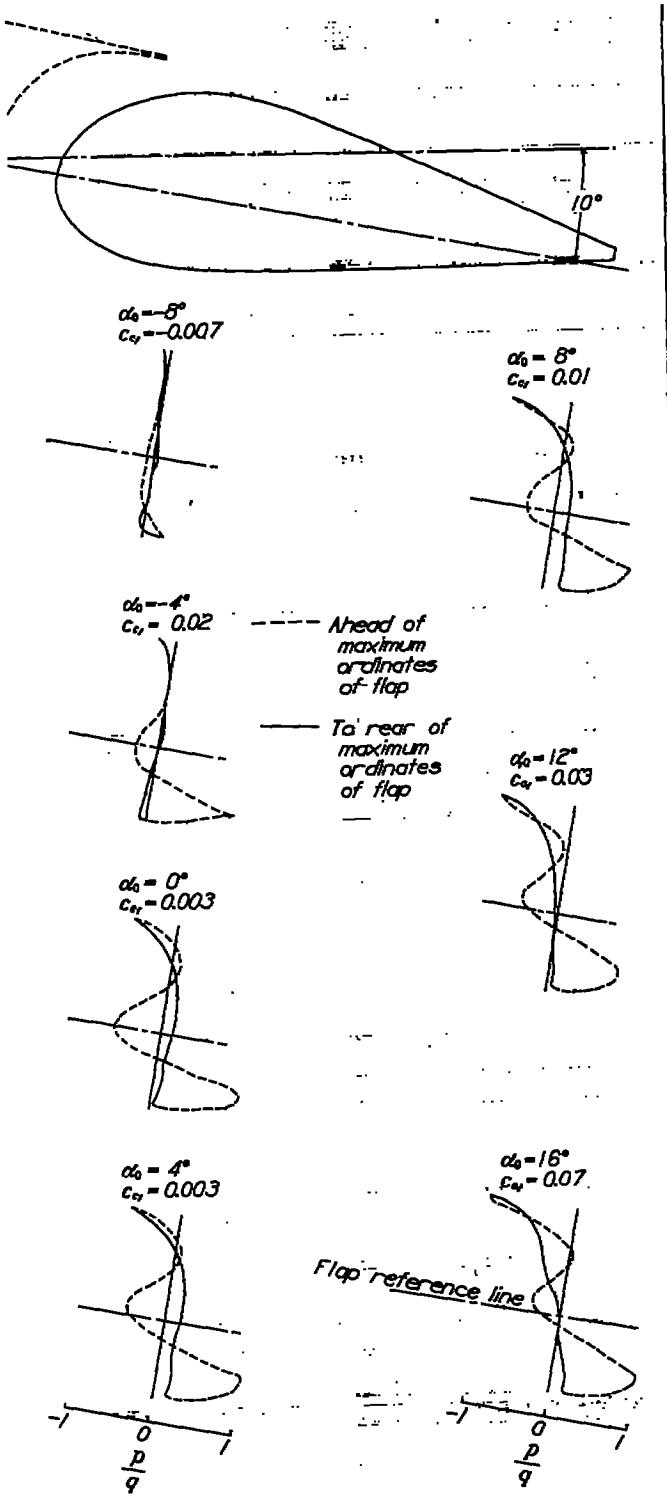

FIGURE 9.—Chord pressure distribution on a 0.25$6c$ slotted flap mounted on the NACA 23021 airfoil. Flap set at 10°.

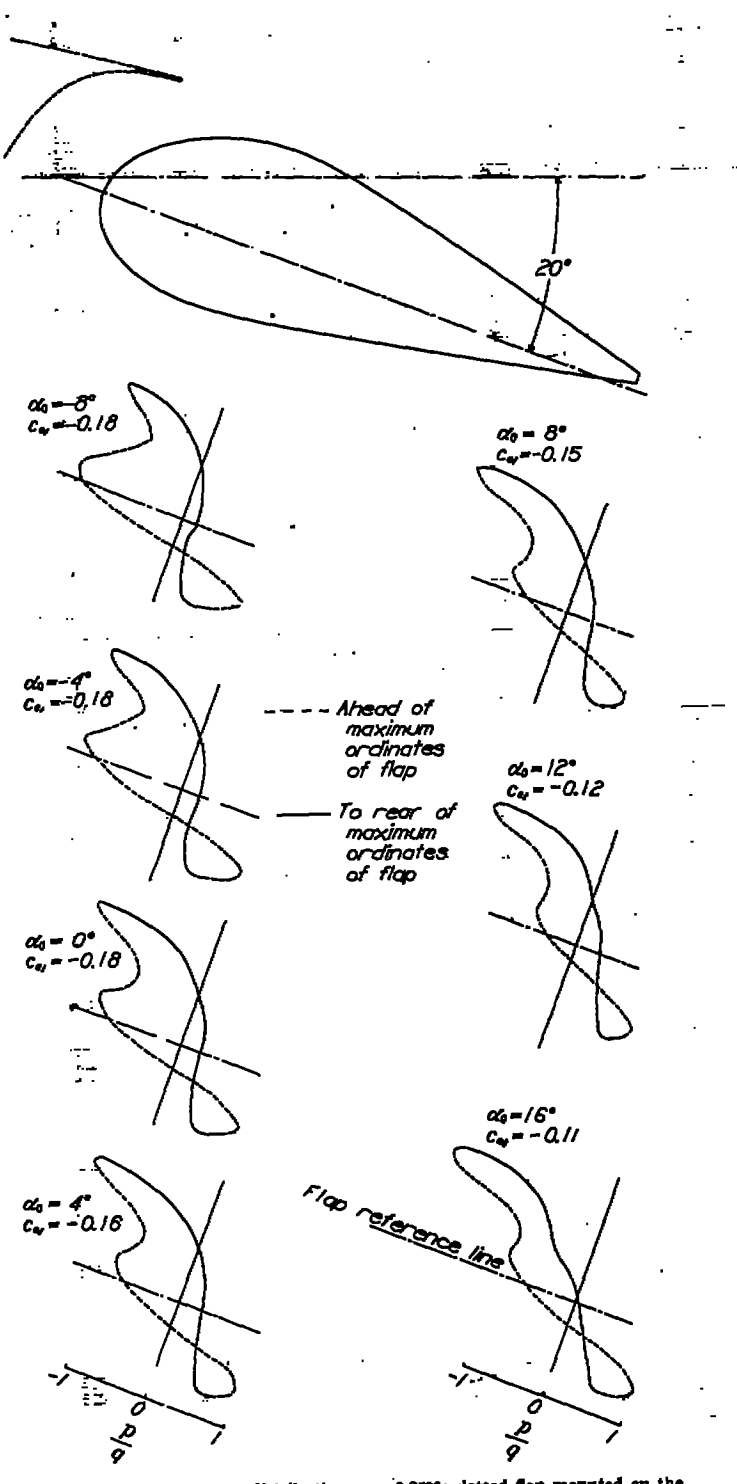

FIGURE 10.—Chord pressure distribution on a 0.25$6c$ slotted flap mounted on the NACA 23021 airfoil. Flap set at 20°.

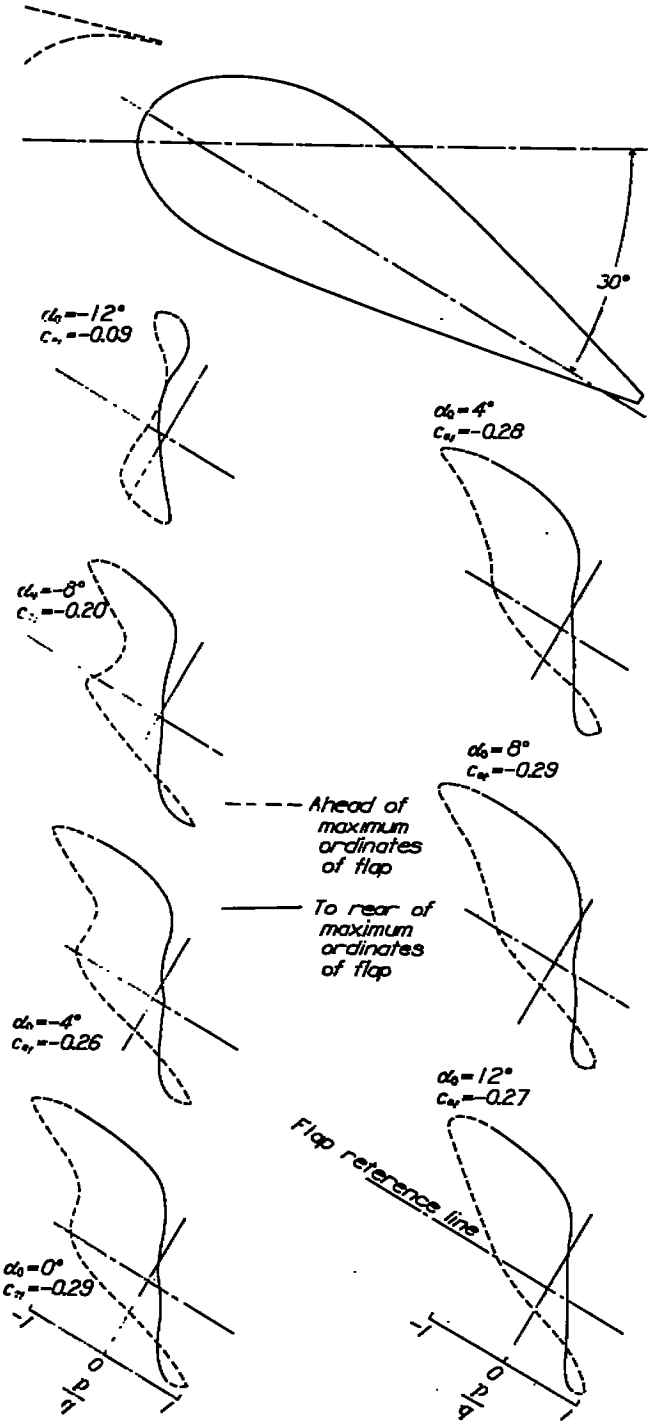

FIGURE 11.—Chord pressure distribution on a 0.256c slotted flap mounted on the NACA 23021 airfoil. Flap set at 30°.

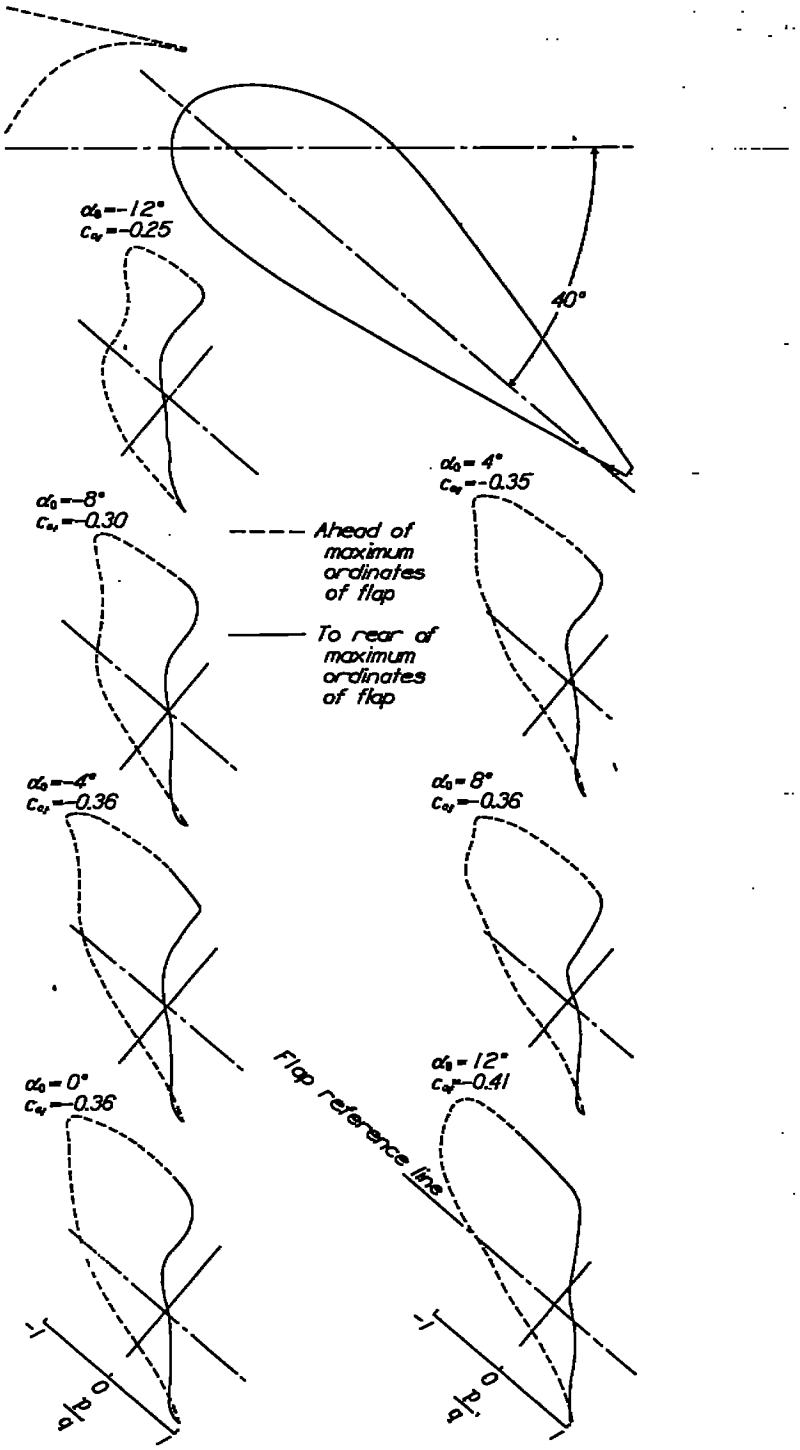

FIGURE 12.—Chord pressure distribution on a 0.256c slotted flap mounted on the NACA 23021 airfoil. Flap set at 40°.

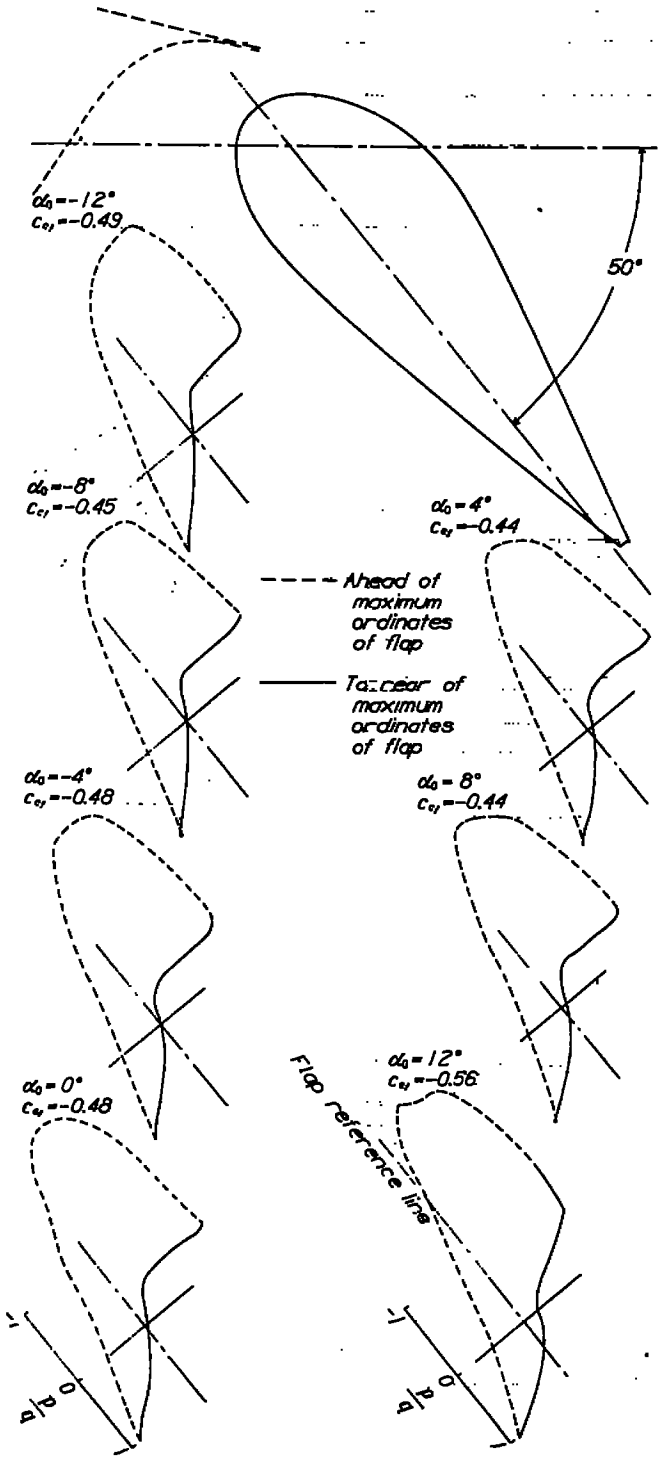

FIGURE 13.—Chord pressure distribution on a 0.266c slotted flap mounted on the NACA 23021 airfoil. Flap set at 30°.

PRECISION

No air-flow alinement tests were made in the tunnel with the test arrangement used in the present investigation. The absolute angle of attack may therefore be in error, but the relative angles of attack of the model are accurate to within ±0.1°. The flaps were set at specified angles to within ±0.5°. The results from check tests, in which both the angle of attack and the flap setting were independently changed, show that the orifice pressures agree within ±2 percent, with the exception of upper-surface pressures near the leading edges which, at high angles of attack, checked within about ±5 percent. The individual free-stream dynamic pressures are accurate to within ±1 percent. A tunnel-wall correction (reference 11) has been applied only to the normal-force coefficients of the airfoil-flap combination. This correction tends to reduce the magnitude of the pressure; the other results, which are uncorrected, should therefore be conservative.

DISCUSSION

SECTION PRESSURE DISTRIBUTION

The pressure curves (figs. 3 to 21) show the distribution of load over the upper and the lower surfaces of the airfoil-flap combinations for several flap deflections. These curves may be applied to the design of ribs and flaps and are also useful for showing the change in distribution of pressure over the airfoil as the flap is deflected. In general, these curves are similar in shape and magnitude to the ones obtained from pressure-distribution investigations of the thinner airfoil-flap combinations (references 3 and 6).

The shapes of the pressure curves for the slotted flap (figs. 3 to 8) are generally similar to those of the curves for the NACA 23012 airfoil with a slotted flap (reference 3); this similarity shows that the flaps have the same characteristics as to extent of peak pressures, occurrence of double peak pressures on the upper surface, and magnitude of peak negative pressures. In the present investigation, the double peak disappeared at flap deflections of 30°.

Figures 3 to 8 show an increase in velocity at the slot entry. In some cases, this velocity exceeds the free-stream velocity; however, the area of increased velocity is small because the deflected flap retards the flow to the rear of the slot.

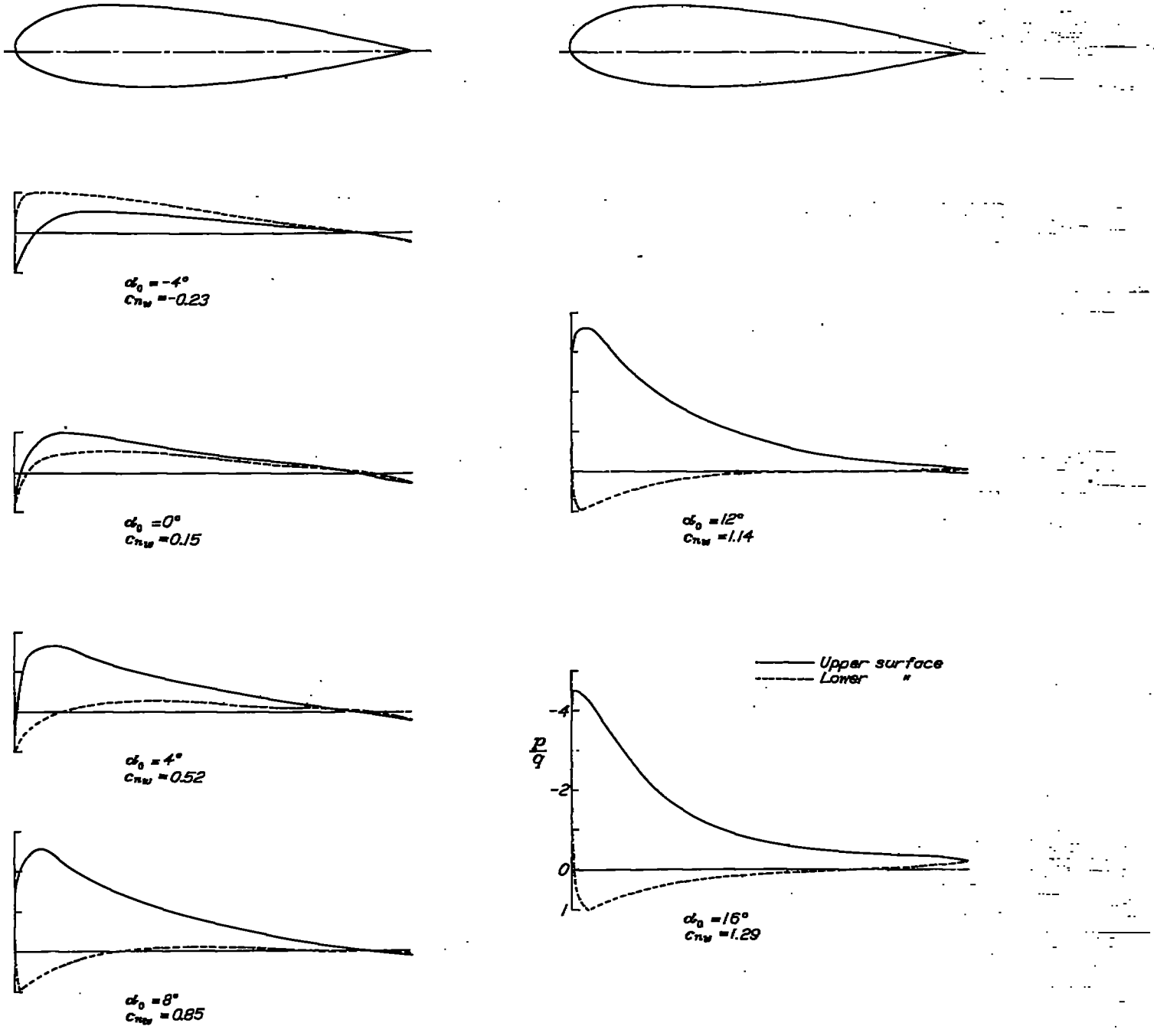

FIGURE 14.—Pressure distribution on the NACA 23021 airfoil with a 0.20c split flap at various angles of attack Flap set at 0°.

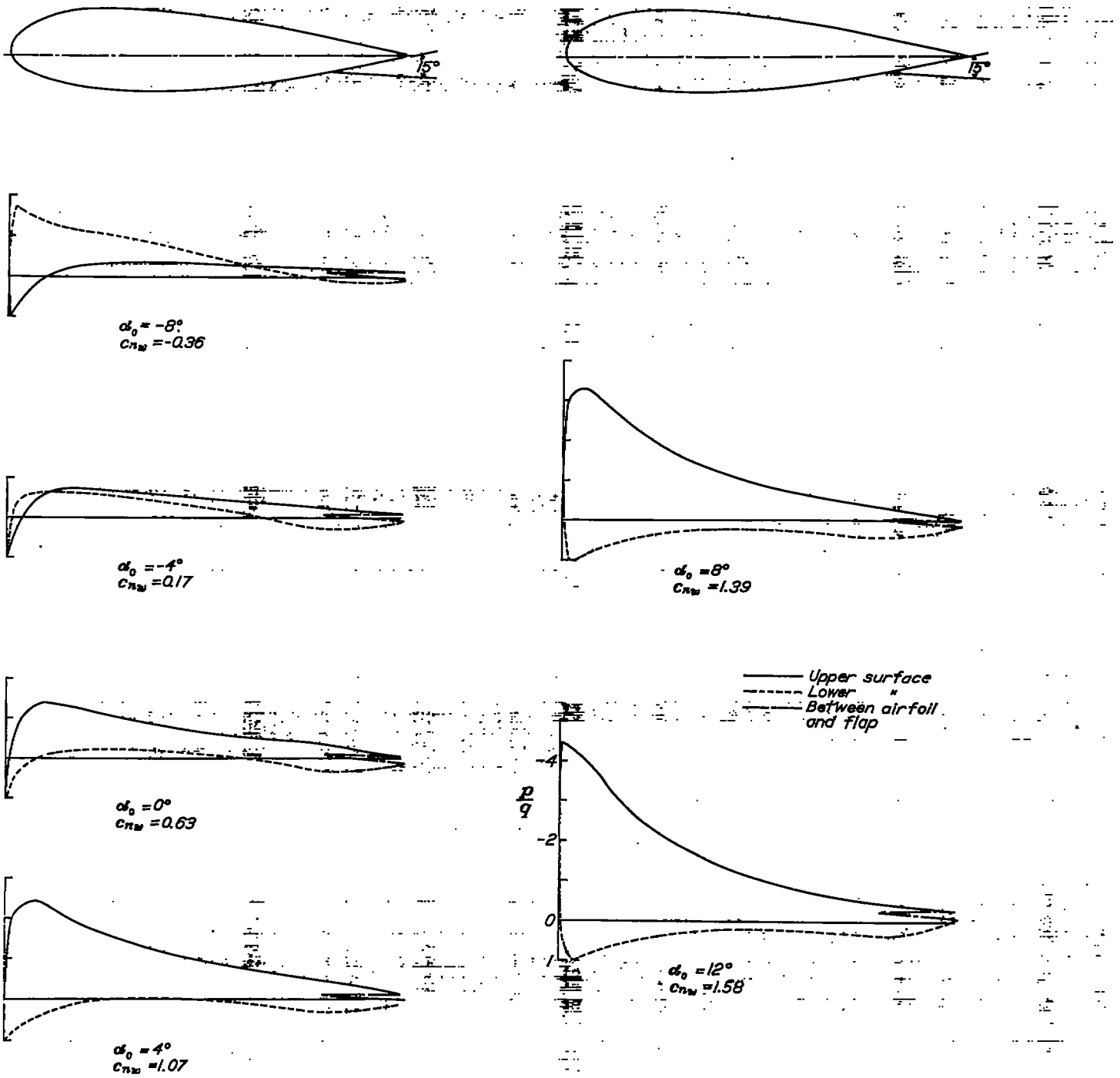

FIGURE 15.—Pressure distribution on the NACA 23021 airfoil with a 0.20c split flap at various angles of attack. Flap set at 15°.

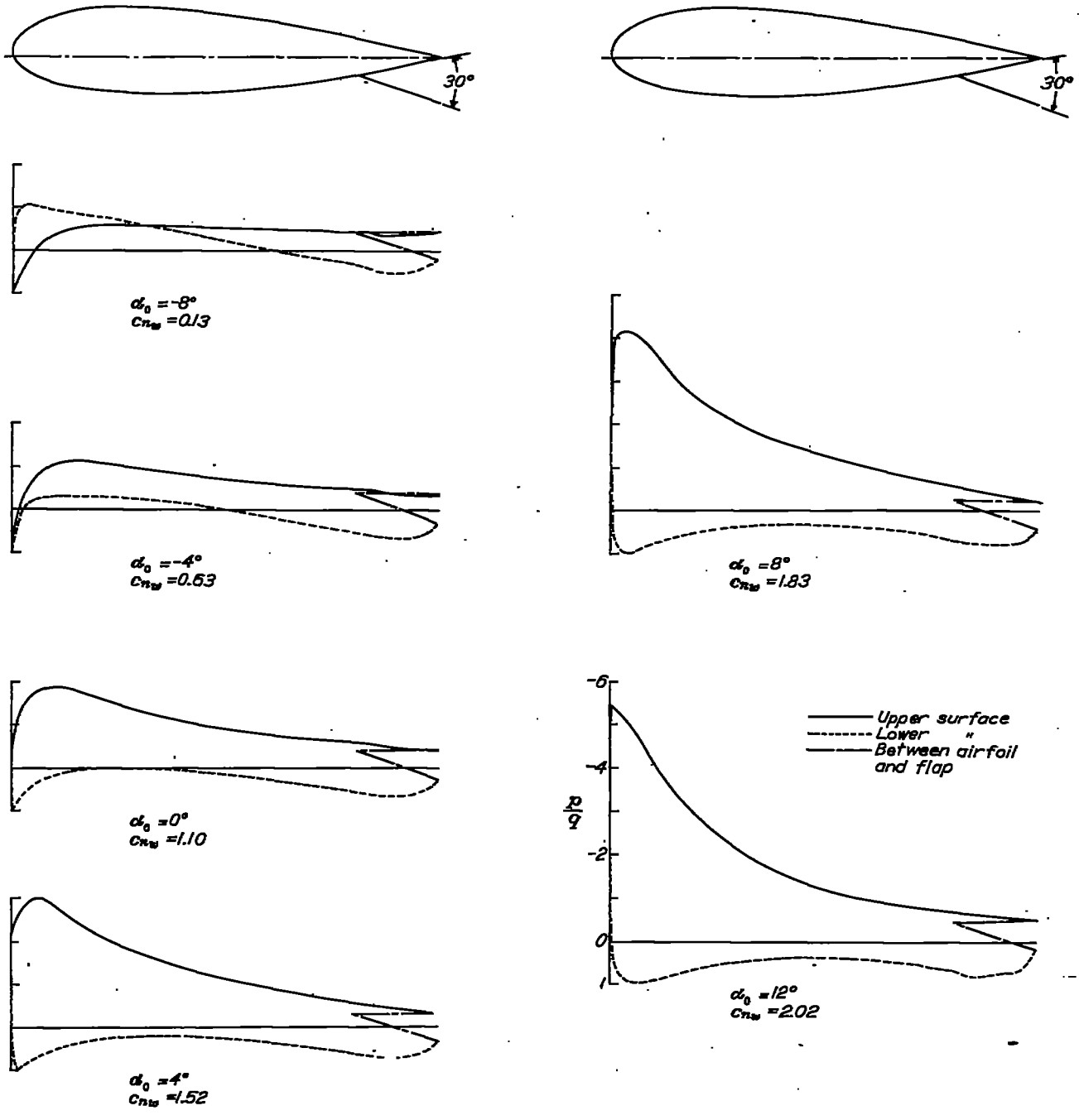

FIGURE 16.—Pressure distribution on the NACA 23021 airfoil with a 0.30c split flap at various angles of attack. Flap set at 30°.

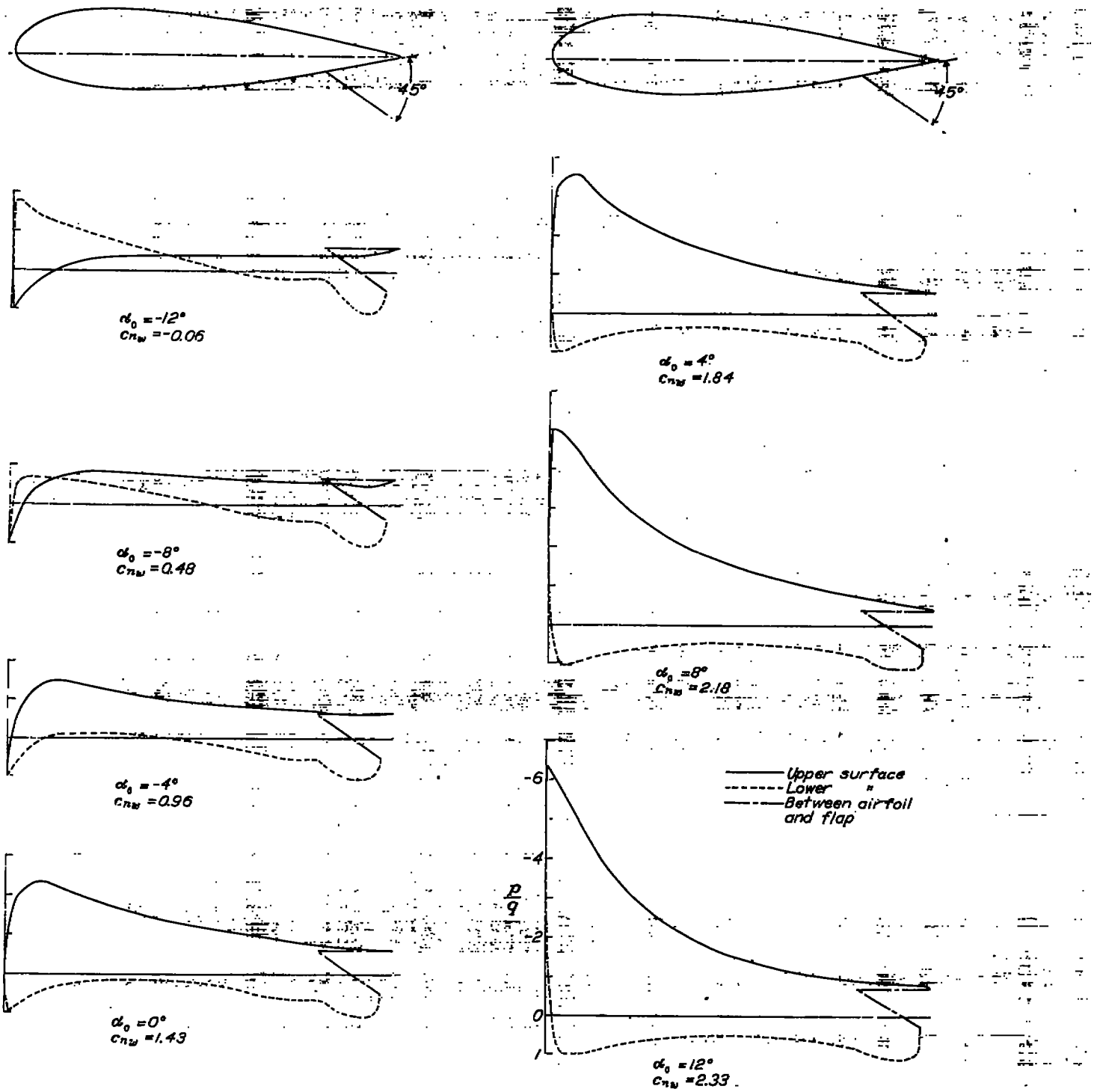

FIGURE 17.—Pressure distribution on the NACA 23021 airfoil with a 0.30c split flap at various angles of attack. Flap set at 45°.

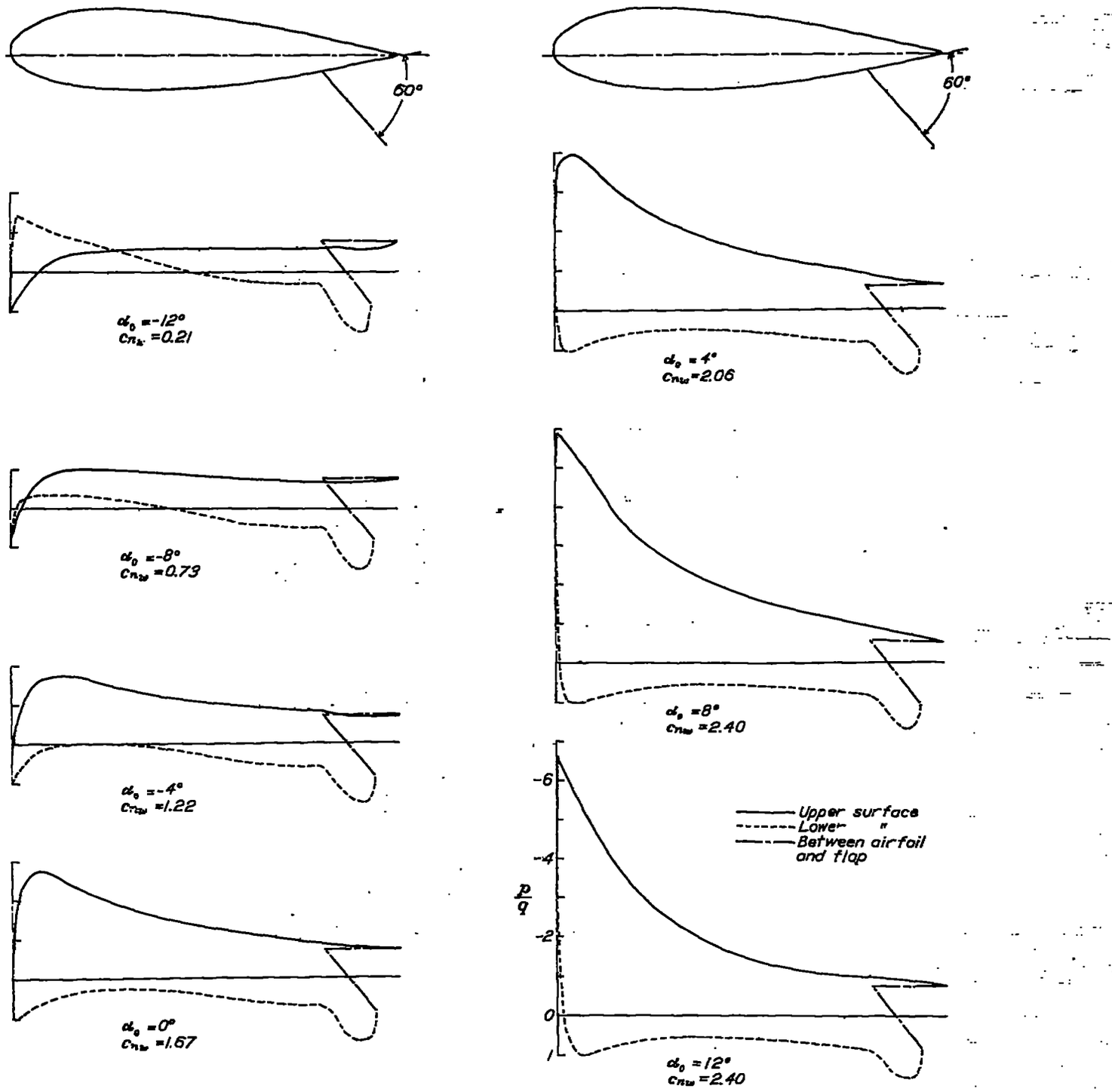

FIGURE 18.—Pressure distribution on the NACA 23021 airfoil with a 0.20c split flap at various angles of attack. Flap set at 60°.

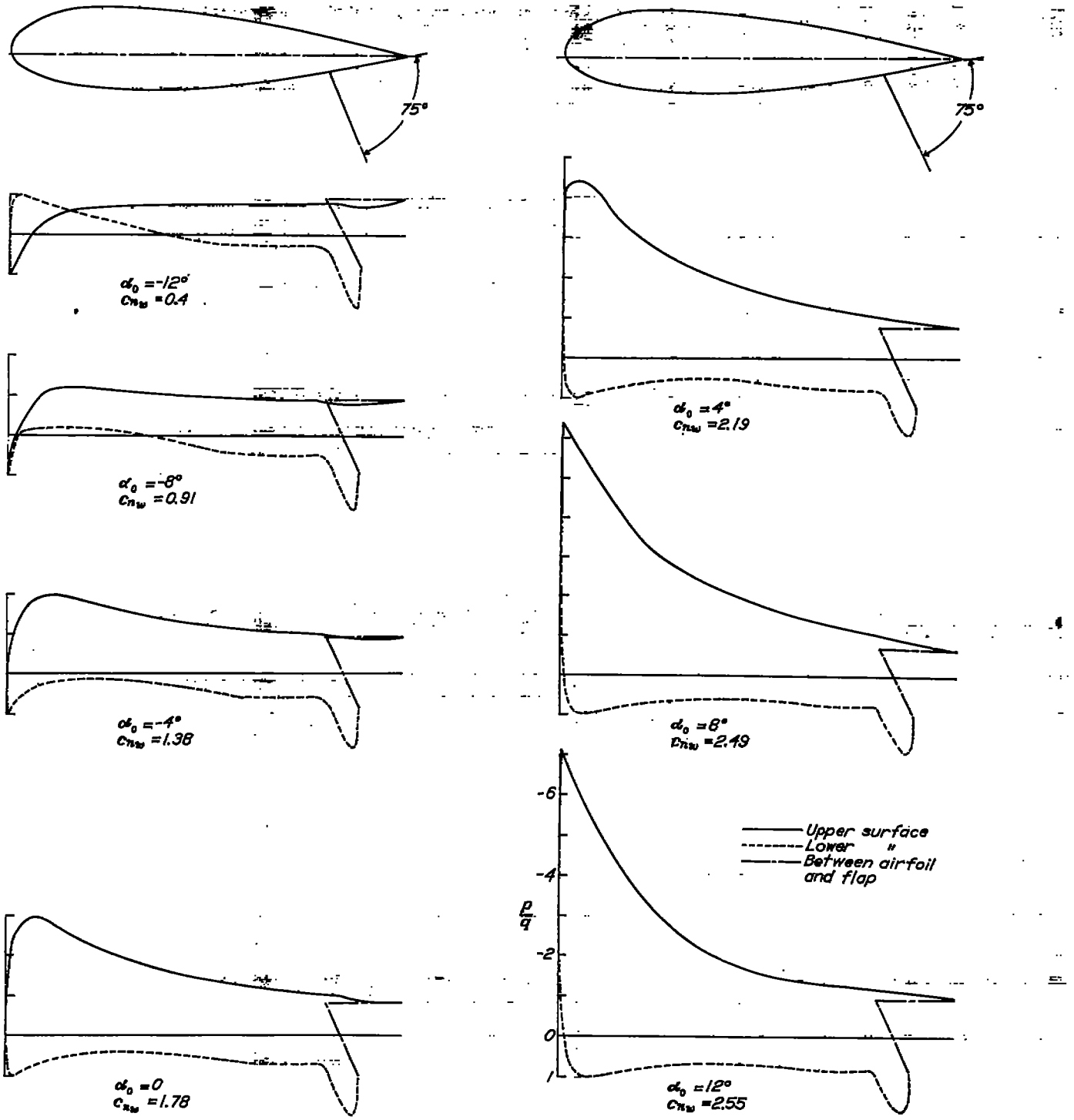

FIGURE 19.—Pressure distribution on the NACA 23021 airfoil with a 0.20c split flap at various angles of attack. Flap set at 75°.

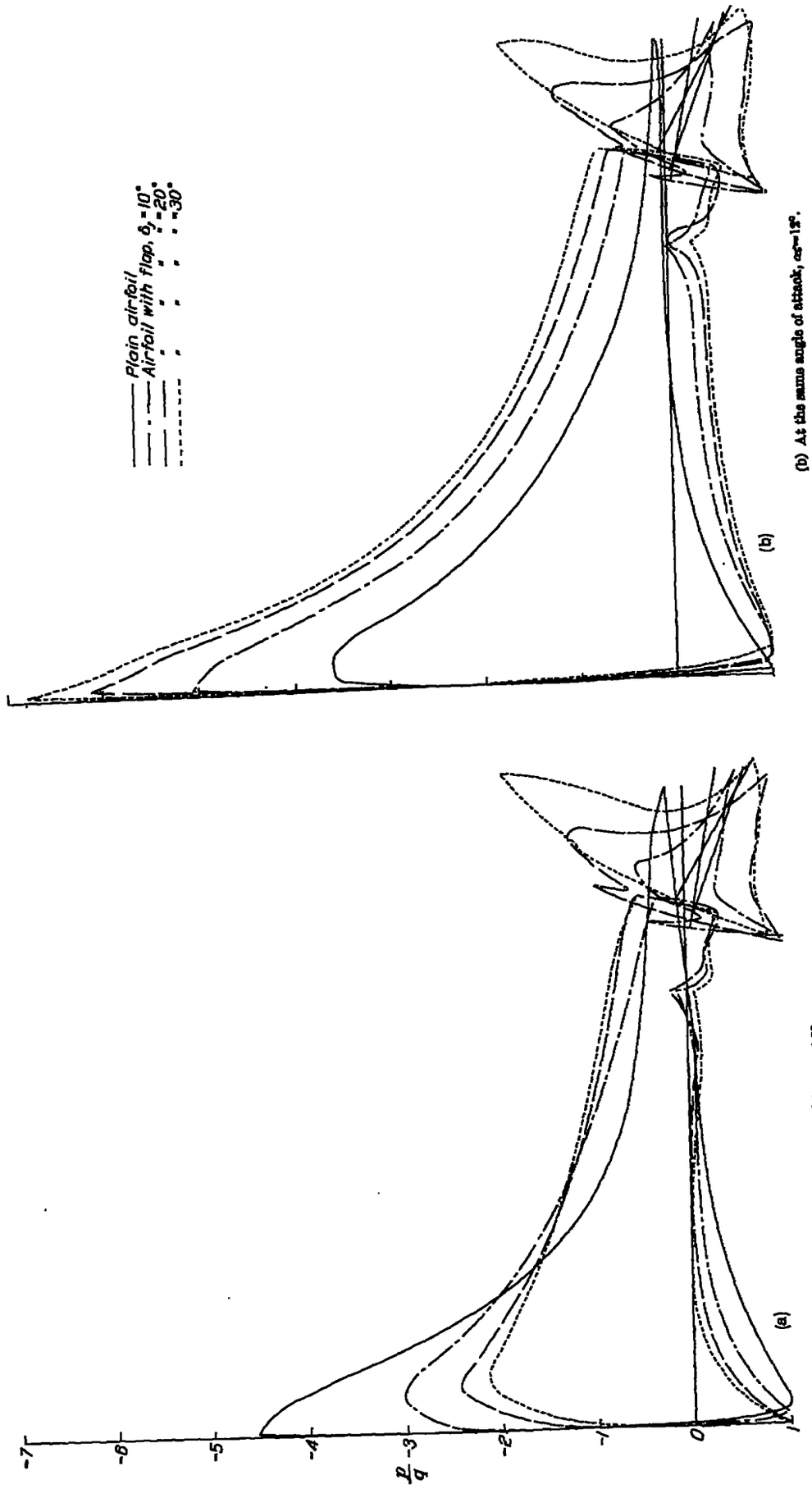

(a) At the same lift, c_{m_0} = -1.20.

(b) At the same angle of attack, α_0 = 12°.

FIGURE 21.—Comparison of the pressure distribution on the NACA 23021 airfoil and a 0.250c slotted flap with that on a plain airfoil.

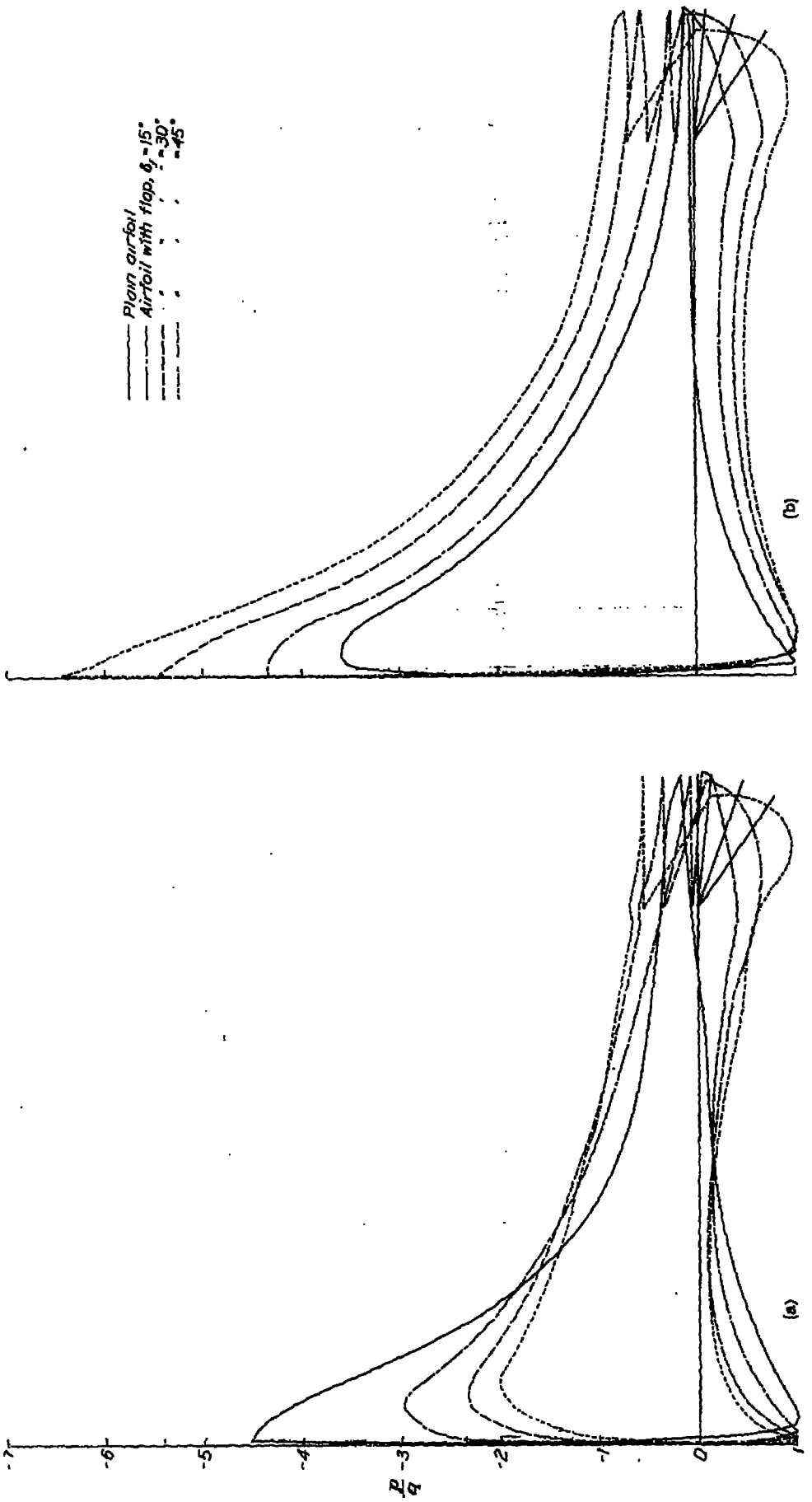

(a) At the same lift, c_l=1.28.

(b) At the same angle of attack, α_g=15°

FIGURE 21.—Comparison of the pressure distribution on the NACA 23021 airfoil and a 0.30c split flap with that on a plain airfoil.

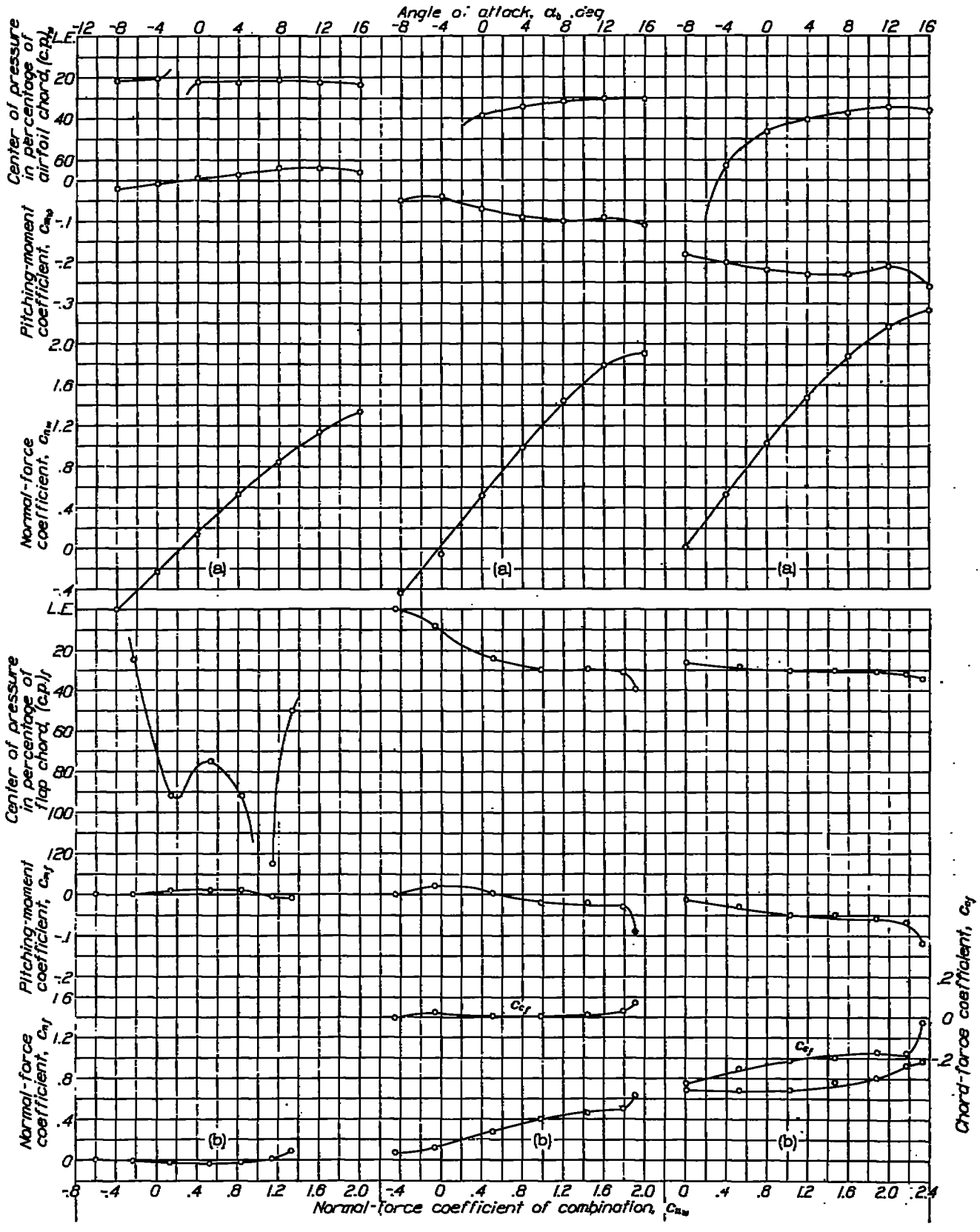

(a) Airfoil with flap. (b) Flap alone.

FIGURE 22.—Flap set at 0°. FIGURE 23.—Flap set at 10°. FIGURE 24.—Flap set at 20°.

Section characteristics of the NACA 23021 airfoil with a 0.250c slotted flap.

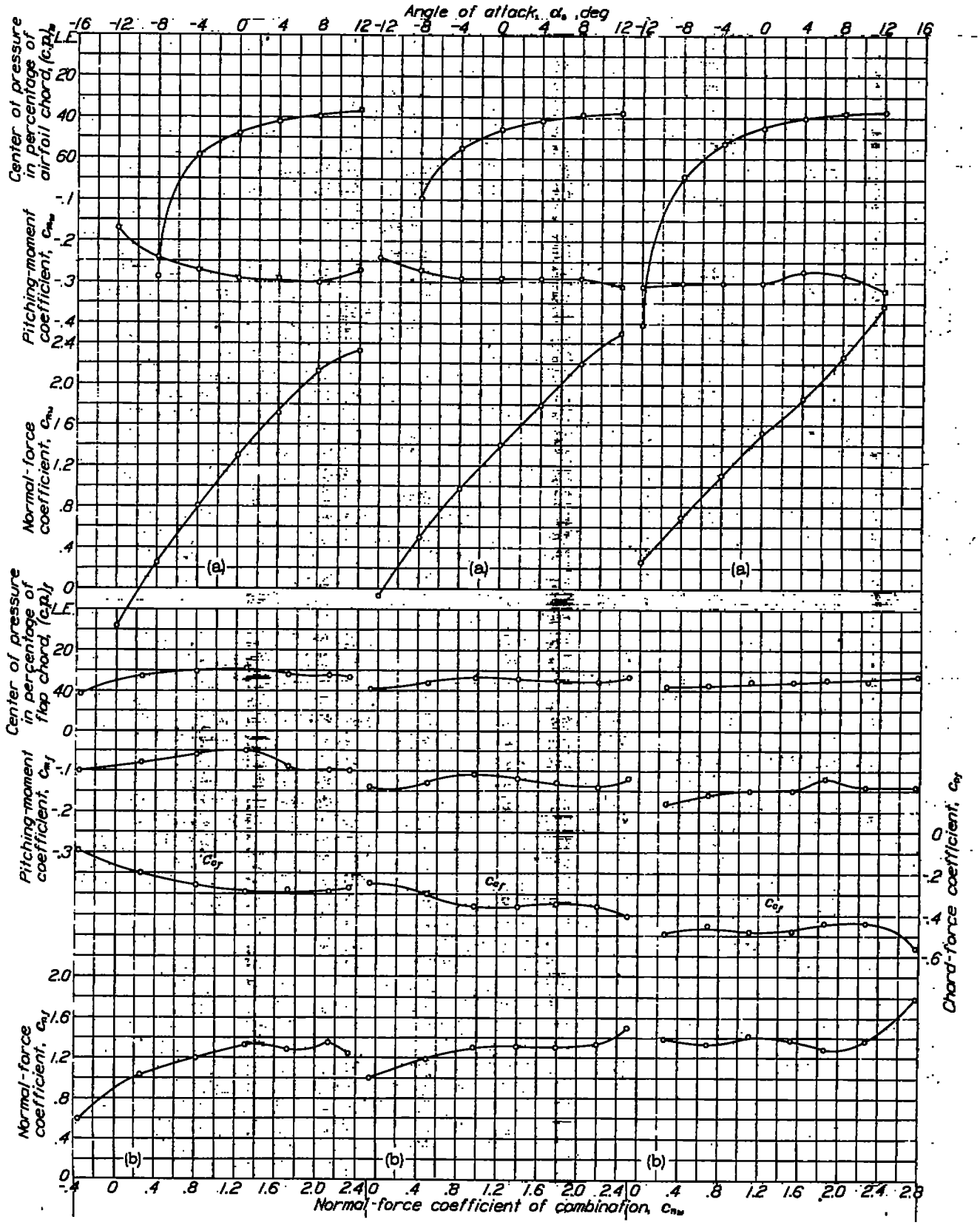

(a) Airfoil with flap.

(b) Flap alone.

FIGURE 25.—Flap set at 30°.

FIGURE 26.—Flap set at 40°.

FIGURE 27.—Flap set at 50°.

Section characteristics of the NACA 23021 airfoil with a 0.250c slotted flap.

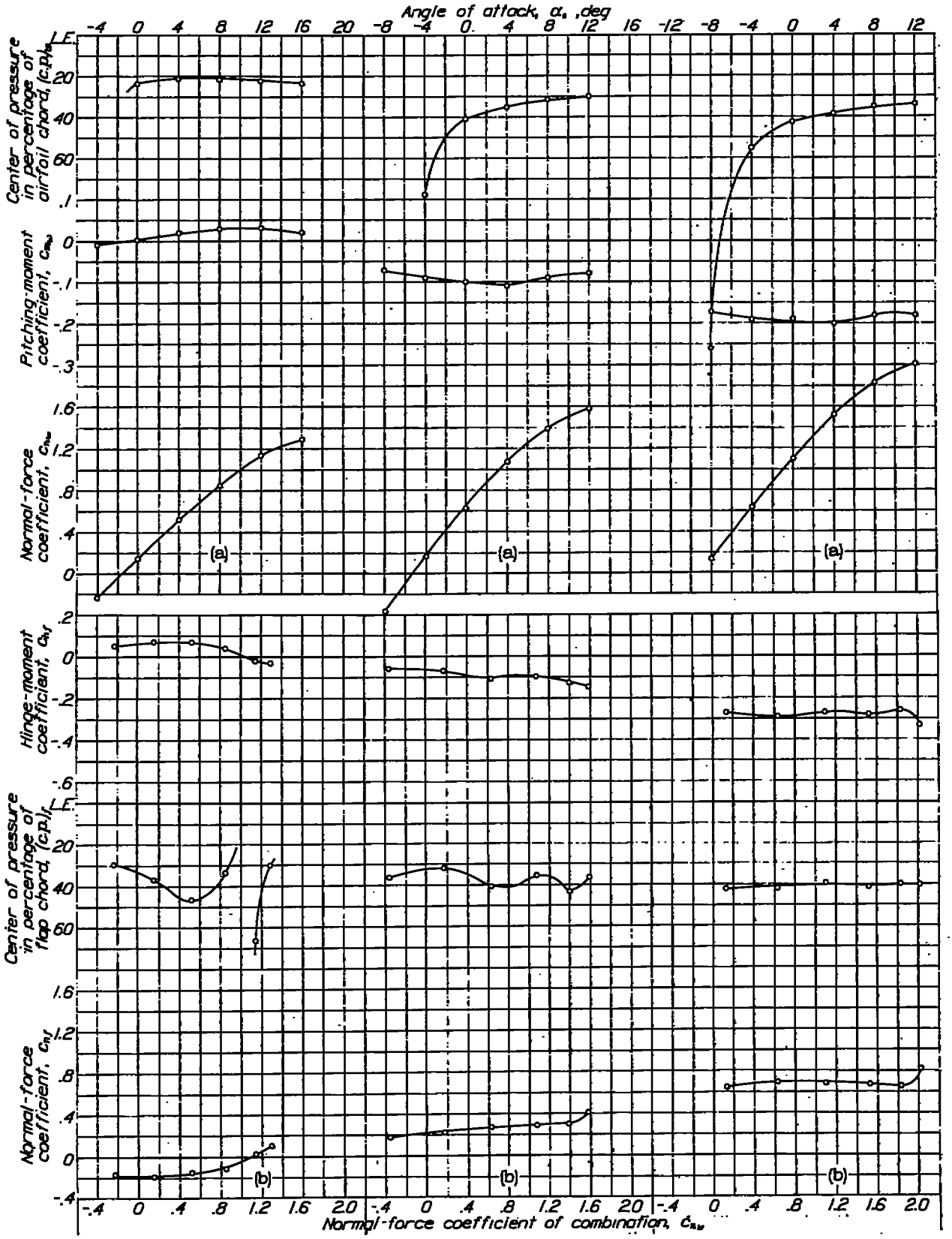

(a) Airfoil with flap.

(b) Flap alone.

FIGURE 28.—Flap set at 0°. FIGURE 29.—Flap set at 15°. FIGURE 30.—Flap set at 30°.

Section characteristics of the NACA 23021 airfoil with a 0.20c split flap.

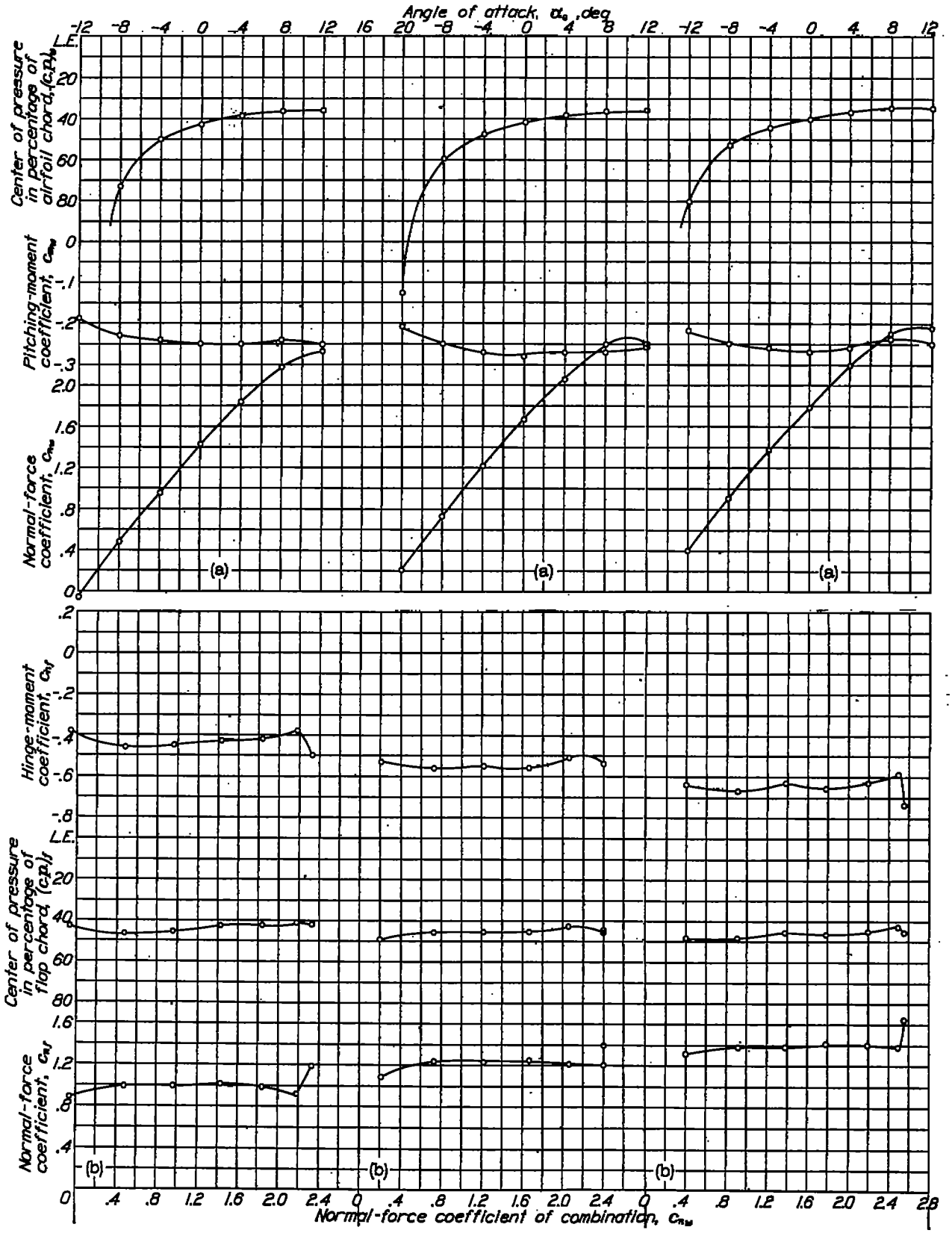

(a) Airfoil with flap. (b) Flap alone.

FIGURE 31.—Flap set at 45°. FIGURE 32.—Flap set at 60°. FIGURE 33.—Flap set at 75°.

Section characteristics of the NACA 23021 airfoil with a 0.20c split flap.

The chord-pressure diagrams (figs. 9 to 13) were included to show that relatively high forces existed which would tend to retract the flap from the maximum-lift setting, as was found for the NACA 23012 airfoil with slotted flap. (See reference 3.) The negative components overbalance the positive ones for almost all flap settings, which creates a force forward. The skin-friction force, if taken into account, will reduce all negative values and increase all positive values because it acts nearly parallel to the chord and to the rear.

No tests were made to determine the effect of a slight deviation from the optimum nose path for the slotted flap but, as pointed out in reference 1, a slight deviation should only slightly change the characteristics. If the change in characteristics is small, there should be little change in the pressure distribution.

A comparison of the pressure distribution over a Fowler, a plain, and an external-airfoil flap with a slotted flap is given in reference 3. As no great differences exist between the curves in reference 3 and those of the present investigation, no comparison with other types of flap is made.

The shapes of the pressure curves for the split flap (figs. 14 to 19) are very similar to the shapes of the curves shown in references 5, 6, and 7. This agreement was expected because reference 4 shows that, with a 0.20c split flap, the maximum lift is practically independent of the airfoil thickness.

Comparison of the pressure diagrams for the plain airfoil with those for the airfoil-flap combinations at the same lift (figs. 20 (a) and 21 (a)) shows that decreasing the angle of attack and increasing the flap angle had the following effects: The pressure at the nose of the airfoil decreased as the flap angle was increased. The negative pressures at the trailing edge were increased for both flap combinations. The positive pressures on the rear part of the split-flap combination increased, but there was little variation in the same region for the slotted-flap combination. The flap loads on both combinations increased with flap angle.

Comparison of the pressure diagrams for the plain airfoil with those for the airfoil-flap combinations at the same angle of attack (figs. 20 (b) and 21 (b)) shows that increasing the flap angle had the following effects: The pressure over the entire combination increased, causing the airfoil to carry a much greater load. The pressure gradient remained about the same throughout the range of flap angles shown. The loads on the flap increased with flap deflection.

The shapes of the pressure curves for the slotted flap are similar to the shapes of the pressure curves for the airfoil alone. The wake of the flap as well as of the combination should therefore be narrow, which accounts for the low drag of the slotted-flap combination as shown in the results reported in reference 1.

Figures 20 and 21 show that the main effect of either flap on the airfoil is its ability to change the flow around the airfoil in such a manner as to decrease the adverse pressure gradient and to cause the airfoil to carry a much greater load without stalling.

AERODYNAMIC SECTION CHARACTERISTICS

A comparison of the section characteristics of the flap alone and of the combination (figs. 22 to 33) shows that the loads on the flap build up more slowly than do the loads on the combination. The loads on the slotted flap (figs. 22 to 27) build up more rapidly with flap deflection than do the loads on the split flap (figs. 28 to 33) and reach a higher maximum value. The

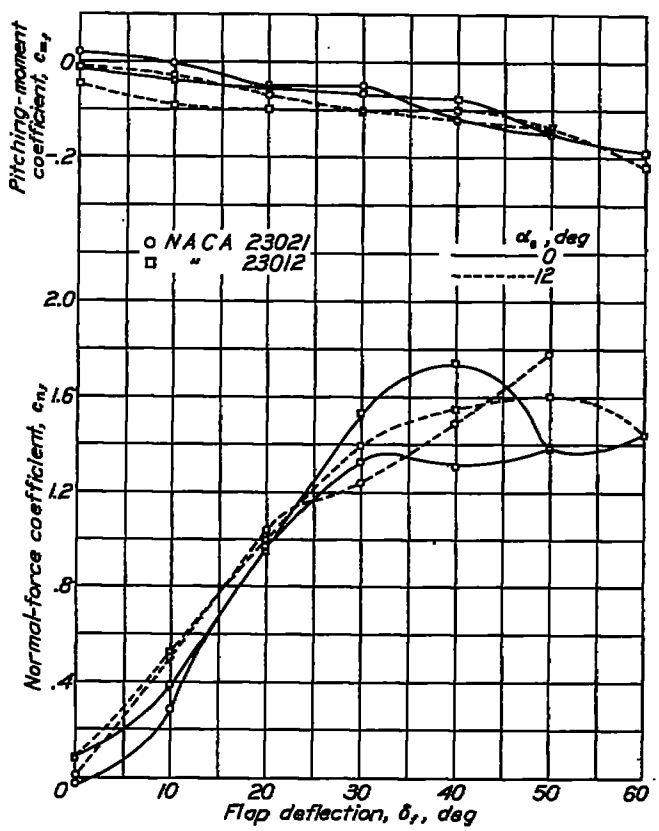

FIGURE 34.—Comparison of section normal-force and pitching-moment coefficients of 0.2566c slotted flap on NACA 23021 and 23012 airfoils.

greater part of the increment of section normal-force coefficient on the combination is the result of the increased load taken by the airfoil. For the slotted-flap combination, approximately 75 percent of the load increment is taken by the airfoil.

The chord-force coefficients of the slotted flap (figs. 22 to 27) are practically all negative in sign; that is, the force acting parallel to the flap reference line is directed forward. The magnitude of these forces is greater than for the NACA 23012 airfoil-flap combination (reference 3). In the calculation of the resultant force on the slotted flap, the chord forces should be taken into account but it should be remembered that these forces do not include skin friction.

The hinge-moment coefficients for the split flap on the NACA 23021 airfoil are slightly greater than those found for the split flap on the thinner airfoils (references 5, 6, and 7). In addition, for both thin and thick airfoils, the hinge-moment coefficients for the split flaps are much greater than the pitching-moment coefficients for the slotted flap, which are about the flap quarter-chord point.

The comparison of the slotted flap on the NACA 23021 airfoil and a similar slotted flap on the NACA 23012 airfoil given in figures 34 and 35 should be useful

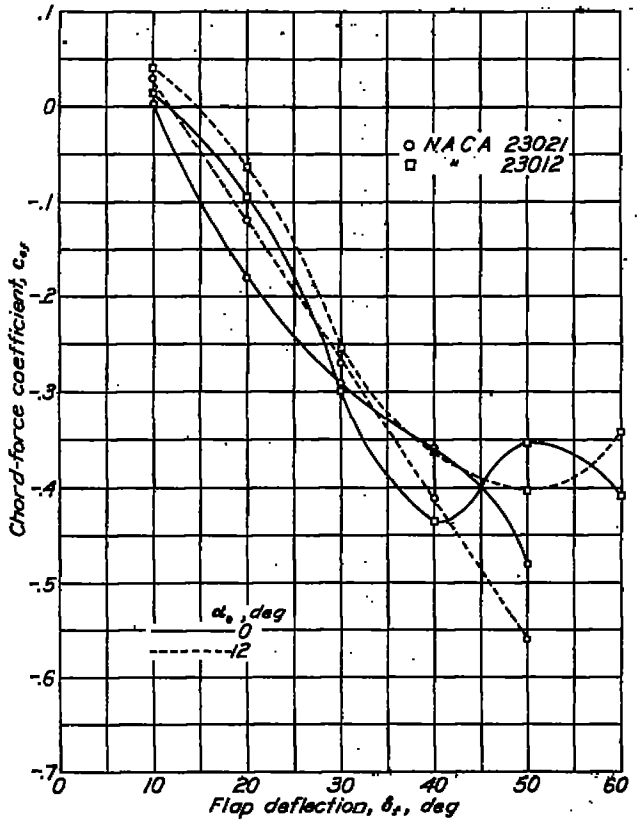

FIGURE 35.—Comparison of section chord-force coefficients of 0.266c slotted flap on NACA 23021 and 23012 airfoils

for the interpolation of flap characteristics for similar slotted flaps on other NACA airfoils of the 230 series. Figure 34 shows the relation between section normal-force and pitching-moment coefficients of the flaps for the two combinations at a low angle of attack, $\alpha_0=0°$, and at a high angle of attack, $\alpha_0=12°$. The normal-force coefficients are approximately the same for the two flaps until the flap deflection exceeds 25°. At low angles of attack, the slotted flap on the NACA 23012 airfoil carries more load for flap deflections greater than 25° but, at high angles of attack, the loads remain about the same throughout the useful range for the flaps on either airfoil. The curves of pitching-moment coefficient show little difference throughout the range tested. A comparison of the section chord-force coefficients (fig. 35) shows the flap on the thinner airfoil to have less chord force in almost all conditions tested. At the high angle of attack, the chord-force coefficient of the slotted flap on the NACA 23021 airfoil is proportional to the flap deflection.

CONCLUSIONS

A comparison of the results for the slotted flap on an NACA 23021 airfoil with the results of pressure-distribution tests of an NACA 23012 airfoil in combination with a slotted flap showed: The flap normal-force coefficients were approximately the same at a high angle of attack over the useful range of flap deflections. The flap pitching-moment coefficients were about the same for the range tested. The chord-force coefficient was higher for most conditions tested for the flap on the NACA 23021 airfoil. The results for the split flap were about the same as previous results for split flaps on thinner airfoils.

LANGLEY MEMORIAL AERONAUTICAL LABORATORY,
NATIONAL ADVISORY COMMITTEE FOR AERONAUTICS,
LANGLEY FIELD, VA., *May 28, 1940.*

REFERENCES

1. Wenzinger, Carl J., and Harris, Thomas A.: Wind-Tunnel Investigation of an N. A. C. A. 23021 Airfoil with Various Arrangements of Slotted Flaps. Rep. No. 677, NACA, 1939.
2. Kiel, Georg: Pressure Distribution on a Wing Section with Slotted Flap in Free Flight Tests. T. M. No. 835, NACA, 1937.
3. Wenzinger, Carl J., and Delano, James B.: Pressure Distribution over an N. A. C. A. 23012 Airfoil with a Slotted and a Plain Flap. Rep. No. 633, NACA, 1938.
4. Wenzinger, Carl J., and Harris, Thomas A.: Wind-Tunnel Investigation of N. A. C. A. 23012, 23021, and 23030 Airfoils with Various Sizes of Split Flap. Rep. No. 668, NACA, 1939.
5. Wallace, Rudolf: Investigation of Full-Scale Split Trailing-Edge Wing Flaps with Various Chords and Hinge Locations. Rep. No. 539, NACA, 1935.
6. Wenzinger, Carl J.: Pressure Distribution over a Clark Y-II Airfoil Section with a Split Flap. T. N. No. 627, NACA, 1937.
7. Wenzinger, Carl J., and Harris, Thomas A.: Pressure Distribution over a Rectangular Airfoil with a Partial-Span Split Flap. Rep. No. 571, NACA, 1936.
8. Wenzinger, Carl J.: Pressure Distribution over an N. A. C. A. 23012 Airfoil with an N. A. C. A. 23012 External-Airfoil Flap. Rep. No. 614, NACA, 1938.
9. Wenzinger, Carl J., and Harris, Thomas A.: The Vertical Wind Tunnel of the National Advisory Committee for Aeronautics. Rep. No. 387, NACA, 1931.
10. Street, William G., and Ames, Milton B., Jr.: Pressure-Distribution Investigation of an N. A. C. A. 0009 Airfoil with a 50-Percent-Chord Plain Flap and Three Tabs. T. N. No. 734, NACA, 1939.
11. Wenzinger, Carl J., and Harris, Thomas A.: Wind-Tunnel Investigation of an N. A. C. A. 23012 Airfoil with Various Arrangements of Slotted Flaps. Rep. No. 664, NACA, 1939.